Physiol Rev
83: 933–963, 2003; 10.1152/physrev.00034.2002.

Oxygen Gradients in the Microcirculation

AMY G. TSAI, PAUL C. JOHNSON, AND MARCOS INTAGLIETTA

Department of Bioengineering, University of California, San Diego, La Jolla, California

Tsai, Amy G., Paul C. Johnson, and Marcos Intaglietta. Oxygen Gradients in the Microcirculation. *Physiol Rev* 83: 933–963, 2003; 10.1152/physrev.00034.2002.—As arterialized blood transits from the central circulation to the periphery, oxygen exits through the vessel walls driven by radial oxygen gradients that extend from the red blood cell column, through the plasma, the vessel wall, and the parenchymal tissue. This exit determines a longitudinal gradient of blood oxygen saturation whose extent is inversely related to the level of metabolic activity of the tissue, being small for the brain and considerable for skeletal muscle at rest where hemoglobin is only half-saturated with oxygen when blood arrives to the capillaries. Data obtained by a variety of methods show that the oxygen loss is too great to be explained by diffusion alone, and oxygen gradients measured in the arteriolar wall provide evidence that

this structure in vivo is a very large oxygen sink, and suggests a rate of oxygen consumption two orders of magnitude greater than seen in in vitro studies. Longitudinal gradients in the capillary network and radial gradients in surrounding tissue also show a dependence on the metabolic rate of the tissue, being more pronounced in brain than in resting skeletal muscle and mesentery. Mean P_{O_2} values increase from the postcapillary venules to the distal vessels of this network while radial gradients indicate additional oxygen loss. This circumstance may be due to pathways with higher flow having higher oxygen content than low flow pathways as well as possible oxygen uptake from adjacent arterioles. Taken together, these newer findings on oxygen gradients in the microcirculation require a reexamination of existing concepts of oxygen delivery to tissue and the role of the capillaries in this process.

I. INTRODUCTION

The circulatory system performs a number of essential functions including delivery of nutrients, removal of waste products, mass transport between organs, communication pathway for the endocrine system, heat exchange with the environment, immunological defense system, and maintenance of fluid balance between blood and the interstitium. On a moment by moment basis however, oxygen delivery to the tissues, especially to the vital organs, is perhaps the most important of these functions. Because the oxygen required by mammalian cells to support metabolism cannot be obtained directly from the environment in sufficient quantity by the process of diffusion, this limitation has been resolved by the evolutionary development of two convective processes driven by an air pump, the lungs, and a fluid pump, the heart. These two processes are regulated so that in the steady state mechanical ventilation delivers oxygen to the blood/gas interface in the lung, the alveolar capillaries, at the same rate that this gas delivered to the tissue by the systemic capillaries is used by metabolic processes in the tissues. The fact that both lung and tissue capillaries possess a vast surface area (126 and 1,200 m^2, respectively, where the disparity in principle reflects a difference of the order of 10 in partial pressure gradient of oxygen between lung and tissue capillaries, Ref. 140) is probably responsible for the conclusion that the two capillary networks represent "mirror images" of each other with the systemic capillaries yielding the oxygen acquired in the lung. The final pathway for oxygen transfer from the alveoli to the blood in the lung and from blood to the parenchymal cells in the tissues supplied by the systemic circulation involves diffusion and is therefore entirely dependent on the gradient for oxygen. Thus a complete picture of the oxygen gradients from blood to tissue is critically important to understanding the process of oxygen delivery to tissue, its capacity, and its limitations. The purpose of this review is to provide an overview of the newer information on oxygen gradients that has become available in recent years, critically examine classical concepts from the perspective of this new information, and suggest appropriate revisions of these concepts.

As blood passes through the lung, oxygen diffuses down its partial pressure gradient from the alveoli into the bloodstream where it combines with hemoglobin in the red blood cells and is carried by convective transport through the heart and large and small arteries to the microcirculatory vessels where the partial pressure gradient favors diffusion from the red blood cell to the tissue. It has been assumed until recently that the unloading of oxygen from the blood to the tissue occurred to a significant degree only in the capillaries. The concept that capillaries are the sole suppliers of oxygen to the tissue is in fact a cornerstone of physiology that became crystallized with the work of Krogh and Erlangen in 1918, who developed the "Krogh cylinder model" (67). With the use of the capillary network of skeletal muscle as an example, this mathematical model describes how oxygen is delivered by a single capillary of a uniform array of capillaries to a surrounding tissue cylinder. At the time this model was developed there were no methods available to determine oxygen levels in the microcirculatory vessels and the tissue. The model therefore assumed that all oxygen exchange takes place at the capillary, with the P_{O_2} at the entrance being that in the large artery and the P_{O_2} at the exit being that in the large vein. This model described longitudinal and radial gradients at the capillary and surrounding tissue and has provided significant insight to the dynamics of oxygen delivery to the tissues. For example, it can be deduced from the model that under conditions of reduced blood flow or arterial oxygen level, the sites in the surrounding tissue cylinder at the greatest radial distance from the venous end of the capillary would be most vulnerable to oxygen lack (50, 68). At the same time, studies of this model have repeatedly noted that it may not fully predict tissue oxygenation (94), due to the underlying heterogeneity of capillary network and hemodynamics. An even more serious issue arises in respect to the assumption that oxygen exchange occurs only at the capillary level. This assumption was perhaps based on the notion that the thickness of the walls of the arterial and venous vessels and the high rate of blood flow would not permit significant loss of oxygen in those regions.

That the Krogh cylinder model has serious limitations as regards the assumed capillary entrance oxygen levels became evident with the advent of methods for localized measurement of microvascular and tissue oxygen levels. It was shown as early as the 1970s that the capillaries are not the only source of O_2 in the microcir-

culation (25) since significant O_2 loss was measured from the arterioles. This key observation did not immediately alter the prevailing concepts of oxygen exchange, perhaps in part because it was based on new methodology. However, subsequent studies by other investigators using polarographic microelectrodes and phosphorescence techniques to determine P_{O_2} and spectrophotometric absorption techniques to determine intravascular hemoglobin saturation have consistently supported the finding that there is significant oxygen loss from the arteriolar network.

The decrease of oxygen content of the blood in the arterioles has been an unresolved problem until recently because the methodology did not reveal the oxygen gradients in the tissues needed to drive the outward flow of oxygen, nor the presence of oxygen sinks that could account for the measured oxygen loss from the arterioles. This situation led to the proposal that the diffusion in the arteriolar wall was an order of magnitude greater than that in tissue (or water) (51) and that the calculations of the oxygen loss had errors that caused a systematic overestimate of the oxygen deficit (135).

The technology now exists for obtaining quantitative information on the different components of the Krogh model, and therefore resolving some of the outstanding questions about how oxygen is managed in the tissue. The method consists of obtaining data that allows us to apply the principle of mass balance to the transport of oxygen in a blood vessel segment. This principle states that the changes in composition or concentration of a substance in a defined region is the sum of the balance between inflow and outflow of the given material from the region plus the amount of material that is either generated or consumed in the same region. Applying this concept to the oxygen transported in a blood vessel segment allows us to write the following relationships

Convective transport = diffusion flux out of the vessel

= oxygen consumed

In this relationship we assume that *1*) the blood vessel is cylindrical, with length L and internal radius R_0; *2*) there are no interactions with other vessels; and *3*) all the oxygen diffusing out is consumed in a tissue region defined by the radius R_t. The convective transport is the total amount of oxygen entering the segment, minus that exiting the segment. The rate at which oxygen is delivered by blood in this segment is given by the product of blood flow Q times the oxygen concentration in blood (neglecting dissolved oxygen) times the change in fractional oxyhemoglobin saturation ΔS, according to the expression

$$QC_{blood}\Delta S = -2\pi R_0 \Delta L D \alpha \frac{dP_{O_2}}{dr}_{r=R_0} = M_{avg}\pi(R_t^2 - R_0^2)\Delta L$$

where the second term is the diffusion flux determined by the diffusion constant D, the oxygen solubility coefficient α, and the radial gradient in the partial pressure of oxygen at the blood/tissue interface. The third term is the oxygen consumed in the perivascular region defined by R_t and the average consumption rate of the cellular components in that region M_{avg}, which includes the endothelium, the vessel wall, and the parenchymal tissue.

This equation summarizes the different components of mass balance that will be discussed in this review, particularly the longitudinal gradients $\Delta S/\Delta L$, which have been measured with several methods that uniformly show that in a number of organs there is a significant exit from the arteriolar segments. New optical methods have produced data that allowed us to characterize radial gradient dP_{O_2}/dr, information that also showed the extend of regional differences of oxygen consumption in the tissue.

Because the interpretation of findings depends somewhat on an understanding of the methods involved and their limitations, we will next address the techniques used in these studies.

II. METHODS FOR MEASUREMENT OF OXYGEN LEVELS IN THE MICROCIRCULATION

A. Polarographic Methods

The polarographic electrode consists of a noble metal membrane-covered cathode where oxygen is reduced and a reference electrode submersed in the medium in which the measurements are to be made. A polarizing voltage causes current to flow in the electrode/medium circuit, where the current-voltage relationship is virtually independent of polarizing voltage in a plateau region of the polarogram. The measuring system is operated at this plateau voltage, where the cathode, an electrode donor, transfers electrons to the oxygen, generating a current proportional to the concentration of oxygen surrounding the electrode and the exposed reactive surface of the electrode. The metal surface is covered with a membrane to prevent the reduction of other molecules in the medium and to reduce the sensitivity to motion of fluid in the immediate vicinity of the electrode. An electrode of this type is usually referred to as a "Clark electrode," which was first described in a patent application (20).

1. Microelectrode techniques

The Clark electrode consumes oxygen generating a current that is the measure of the oxygen concentration in the medium. This current is determined by the oxygen concentration gradient between the electrode metal surface and the medium. This oxygen gradient is located in

the boundary layer near the electrode surface, i.e., the catchment volume; thus any motion of the electrode or medium, or change of medium oxygen concentration, requires that a new stable boundary/diffusion layer be formed before an interpretable oxygen concentration measurement can be made. It is particularly difficult to establish a stable boundary layer at the tip of a microelectrode, which led Whalen et al. (141) to recess the metal surface from the glass micropipette tip, and to fill the tip with collodion, in such a fashion that a motion free layer is always in contact with the metal. Electrodes with tip diameters as small as 1 μm can be made by this process. These electrodes have low drift and oxygen consumption (on the order of 10^{-6} μl/min) and their time constant is of the order of 1 s. They are fragile to use, their introduction into the tissue introduces perturbations, and they become very noisy when used in flowing blood; however, they permit direct visualization of the location of measurement.

It is important to realize that the location of the microelectrode tip defines the center of the catchment volume whose surface P_{O_2} is averaged by the electrode current; therefore, as an example, if the catchment volume includes a portion of an arteriole the current generated and therefore the oxygen measurement will reflect in part the presence of this high oxygen concentration region, even though the oxygen tension at the tip of the electrode may be significantly lower. Oxygen values could be affected significantly by the catchment volume in the case of the oxygen microelectrode method.

Recessed-type electrodes have superior characteristics when compared with exposed cathode electrodes and have advantages that are also reflected in smaller catchment volumes. This parameter is not specifically modeled in most analysis of electrode characteristics; however, it can be in part deduced when the oxygen concentration field around the electrode is known. Schneiderman and Goldstick (106) report the configuration of the oxygen field around the electrode tips with different ratios (l/d) of electrode recession (l, distance between the cathode surface and the tip of the glass micropipette) to electrode diameter (d), showing that shape of field is strongly dependent on this ratio for shallow depths of recession (smaller than the electrode diameter). In the case of exposed electrodes or membrane-covered electrodes, the catchment volume of the electrode is estimated to have a diameter that is about twice the diameter of the exposed area of the electrode (41). When recessed tip electrodes (Whalen electrodes) are used, the catchment volume would appear to be the same for l/d ratios of 0.5 and essentially insignificant for ratios of 5. Therefore, a precise interpretation of the data on tissue oxygen gradient measurement with microelectrodes cannot be made unless the l/d ratio is known.

2. Surface electrodes

The electrical properties of microelectrodes have been improved considerably with the development of surface Clark electrodes where both cathode and anode are sealed by a lipophilic membrane, thus providing a greater protection from impurities and, in principle, eliminating motion artifacts. However, they are implemented with electrodes of ~10–20 μm diameter, increasing the catchment volume to a sphere of 50 μm diameter and the time needed for establishing a stable boundary layer. These sensors are often configured in an array of independently connected sensors, whose signals are used to form a histogram of oxygen tensions. The arrays are calibrated by exposing them to a saline solution equilibrated with N_2 and N_2 + 10% oxygen. The response for each electrode in the array is computer memorized. Calibration is repeated every 3 h and applied to each reading for each electrode assuming linear drift between calibration points (63). These electrodes are placed over the field in which the measurements will be made, without the possibility of intentionally positioning them over specific microvascular structures. Therefore, the information is random and cannot be correlated with the underlying vessel types in the tissue under study. The histogram is obtained by moving the electrode array to multiple locations and is used to define a mean tissue P_{O_2} and the dispersion of tissue P_{O_2}. However, shifting of the electrodes to different locations will not necessarily result in the formation of an identical, stable boundary/diffusion layer in the proximity of the electrode after each relocation, which changes the array calibration. This factor, in addition to the uncertainty of location of the electrodes and the large catchment volume, limits the usefulness of the data.

B. Hemoglobin Spectrophotometric Methods

The partial pressure of oxygen in the blood in microvessels can be determined by a technique that evaluates oxygen saturation of hemoglobin through measurements of light absorption at different wavelengths of the hemoglobin absorption spectrum. This technique has been implemented utilizing two and three wavelengths, where the choice depends on the need to correct for light scattering. This indirect technique is attractive because it utilizes optical means that are easily implemented at the microscope (90). However, with respect to its use to determine P_{O_2}, it depends on a precise knowledge of the hemoglobin absorption spectrum and the relationship between the oxygen dissociation curve for hemoglobin and P_{O_2}, a relation that is strongly influenced by local carbon dioxide concentration and pH, parameters that are not easily determined in blood in the microcirculation. A further limitation of this technique is that it cannot be used to measure tissue P_{O_2}.

The P_{O_2} values obtained with the spectrophotometric technique were found to agree with periarteriolar microelectrode measurements in vivo by Pittman and Duling (90) and Steenbergen et al. (119). The latter group compared periarteriolar P_{O_2} measured with the microelectrode method and the value estimated from oxygen saturation of the red blood cells in the arteriolar lumen of the rat intestine and found a difference of <1 mmHg over a range of 0–100 mmHg. These investigators used microelectrodes of 5- to 8-μm tip diameter, and therefore, as a consequence of the extended catchment volume, their measurements are most likely representative of the P_{O_2} in blood, and not the external wall of the vessel itself.

C. Cryoscopic Hemoglobin and Myoglobin Measurements

Estimates of the level of oxygen in the vascular lumen and parenchymal cells can be obtained by cryoscopic measurements of hemoglobin and myoglobin saturation from thin sections of rapidly frozen tissue as described by Gayeski and Honig (36). In their studies, a copper plate cooled with liquid nitrogen was rapidly applied to the surface of a skeletal muscle, cooling the tissue 500 μm below the surface to the freezing point in 50 ms. Three isosbestic wavelengths and a measuring wavelength in the region of 544–579 nm were used. This method has the advantage that one can obtain measurements at a variety of vascular and tissue sites at a fixed time point, as opposed to the single site measurements possible with in vivo methods. However, the rate of cooling is not sufficient to prevent water crystallization (92), which limits optical resolution and thus the accuracy of oxygen gradient determinations over short distances.

D. Porphyrin Phosphorescence Methods

High spatial resolution measurements of oxygen tension in the microvessels and the surrounding tissue by optical means are now possible through the development of the phosphorescence quenching technique. Because this technique has yielded extensive information on the oxygen gradients in the microcirculation, it will be described here in some detail. The phosphorescence method (114, 115, 129, 136, 142) is based on the relationship between the rate of decay rate of excited phosphorescence from palladium-mesotetra-(4-carboxyphenyl)-porphyrin (Porphyrin Products, Logan, UT) bound to albumin and the partial pressure of oxygen according to the Stern-Volmer equation (136, 142). In this method, animals receive a slow intravenous injection of the porphyrin dye (15 mg/kg body wt) at a concentration of 10 mg/ml ~10 min before P_{O_2} measurements. The dye is made to phosphoresce by excitation with light flashes, and the oxygen concentration in an adjustable optical window that delineates the area where the measurement is to be made is deduced from the rate of decay of the phosphorescence, which depends on the amount of oxygen that surrounds the dye.

Phosphorescence is the emission of photons due to the electronic transition in molecules that are excited into a triplet state by absorbing light and then passing from this state to a singlet ground state (114, 136). Molecules such as Pd-porphyrin either release the absorbed energy as light or transfer this energy to oxygen, which prevents light emission, therefore "quenching" the phosphorescence. The intensity of light emission $I(t)$ from many molecules is described by an exponential decay of the form

$$I(t) = I_0 \exp(-t/a)$$

where I_0 is the maximum intensity at time (t) 0 and a is the decay time constant. When light emission is quenched, fewer photons are emitted, which translates into a shorter time constant a. For quenching to occur it is necessary that the phosphorescent molecule and the quenching agent (oxygen) collide before the occurrence of the triplet to ground state transition, a process that is in part dependent on the abundance (or concentration) of quenchers. The relationship between the decay constant a and oxygen concentration (given by the product of oxygen solubility in the medium, α, and the local partial pressure P_{O_2} of oxygen) is give by the Stern-Volmer equation

$$\tau_0/a = 1 + K_Q \tau_0 \alpha P_{O_2}$$

where τ_0 is the phosphorescence decay constant in absence of oxygen and K_Q is the quenching constant. An advantage of this method is that mixing Pd-porphyrin with excess albumin leads to the formation of a probe whose sensitivity to oxygen quenching is independent of the probe concentration. In other words, the decay constant becomes independent of the concentration of the albumin/porphyrin complex. Another advantage of this method is that calibrations performed in vitro can be subsequently applied to measurements obtained in vivo, since oxygen is the only chemical species that significantly influences the rate of decay of the excited phosphorescence (136).

This method has been used most frequently to determine intravascular microcirculatory blood oxygen levels, starting with the report of Wilson et al. (143), Shonat et al. (115), Torres Filho and Intaglietta (129), Shonat and coworkers (113, 114), Zheng et al. (147), Kerger et al. (62), Sinaasappel et al. (117), and Helmlinger et al. (45). Regarding extravascular measurement, the blood-borne albumin-bound probe passes into the interstitium at a rate

that depends on the reflection coefficient of albumin in the vascular network under study (86). The resulting accumulation of albumin-bound dye within the tissue, which may contain up to 10% of the total albumin in the organism, allows us to measure tissue P_{O_2} at high resolution with the same technique, if the signal-to-noise ratio is adequate.

Phosphorescence generated by the light excitation of the porphyrin probe consumes O_2. The amount consumed depends on the concentration of the dye and the total energy delivered by the light source. With a very intense illumination, it is possible to make a determination of oxygen level with a single flash (147). In this implementation, the flash lamp employed had a 25-μs decay constant which precluded the acquisition of phosphorescence decay data before ~80 μs after flash extinction, and therefore prevented reliable measurements of P_{O_2} above ~50 mmHg, which corresponds to a phosphorescence decay time of the similar duration. The emission obtained with this technique is intense, and the phosphorescence decay curve may be the summation of signals from adjoining areas that would not normally have sufficient intensity to affect the principal component present, particularly if the measurement is made in the neighborhood of a microvessel where the oxygen field is not uniform. In addition, oxygen is consumed as the phosphorescence decays, further distorting the decay signal. These problems have been reported to be amenable to solution by deconvolving the decay signal by mathematical techniques, an approach that may be useful if signal noise is very small (137, 147). Other laboratories have circumvented the problem of oxygen consumption due to the measurement technique by using repeated light excitation of low intensity over a period that allows diffusion to replenish the consumed oxygen, and averaging the signal to obtain the final P_{O_2} measurement (114, 129).

All implementations use a probe injection of 20–30 mg porphyrin/kg body wt, leading to a blood concentration of 0.3 mg/ml, and tissue fluid concentration smaller than 0.1 mg/ml. The multi-flash system of Torres Filho and Intaglietta (129) with a flash decay constant of 10 μs requires 100 flashes to obtain an interpretable signal in blood, where each flash consumes oxygen, causing the concentration of oxygen in stationary plasma to decrease by 0.01 mmHg/flash at steady state. Thus a single flash system that gives an interpretable signal will introduce an error <1 mmHg when used in stationary tissue fluid. This error may be lower in tissue because the amount of probe present is about one-third that of plasma, but this causes a proportional decrease in phosphorescence signal, requiring a significant increase of flash intensity and a corresponding increase in the consumption of oxygen, which may explain why not all systems are able to obtain tissue measurements. Therefore, systems built according to the method of Golub et al. (40) that use few flashes of high intensity and long flash duration are adequate for measurement of intravascular P_{O_2} where the moving blood replenishes the consumed oxygen, if the blood P_{O_2} is low; however, they cannot be used to measure P_{O_2} values greater than about 50 mmHg, since light from the flash illumination is superposed to the phosphorescent emission. Furthermore, this method cannot measure tissue P_{O_2} due to the high oxygen consumption of the flash, a process that affects the signal as the phosphorescence is emitted, introducing a highly variable, dye concentration-dependent perturbation into the measurement.

Comparison of in vivo P_{O_2} measurements at the same site with the multi-flash phosphorescence method and the microelectrode technique were obtained by two groups of investigators using avascular tissue areas of the hamster skinfold preparation (17) and rat skeletal muscle (112). In the hamster preparation superfused with Krebs solution bubbled with 100% N_2, there was a maximum divergence of 2% between the methods over the tissue P_{O_2} range of 5–40 mmHg. Similar results were obtained in rat skeletal muscle over a range of 7–90 mmHg. In addition, multiple excitation of phosphorescence by repeated flashes at a frequency of 30/s over a period of up to 1 min did not produce a detectable change in value obtained with the microelectrode measurement (17).

III. MICROCIRCULATORY PREPARATIONS

A. Surgically Exposed Tissue Preparations

Most of the studies reviewed herein were performed on acutely exposed tissues in anesthetized animals. Pentobarbital sodium is the most commonly used anesthetic, and anesthesia is typically maintained in the surgical plane. However, the precise level of anesthesia may vary among laboratories as well as in a single preparation during the course of an experiment. A commonly used tissue is the cremaster muscle of the rat or the hamster. Surgical preparation involves removal of the skin and exposure of the muscle under a physiological salt solution (PSS) followed by removal of the testicle or moving it up into the body cavity. The animal and muscle are then mounted on a platform which provides an elevated area on which the muscle is spread out for viewing the microcirculatory vessels. PSS equilibrated either with 100% N_2 or with 95% N_2-5% O_2 is usually suffused over the muscle. Such suffusate oxygen levels are found to have minimal effect on the tissue oxygen level as discussed in section x*B*. Some investigators also add 5% CO_2 to the gas mixture if HCO_3-buffered PSS is used. Measurements with the oxygen microelectrode require continuous bathing of the tissue surface with the suffusing solution. While the suffusate solution may affect the degree of hydration of the tissue, it also enables the investigator to alter the oxygen

level at the tissue surface by changing the oxygen concentration of the suffusate. Elevating the oxygen level in the suffusate will increase the degree of arteriolar tone (24, 121) and decrease functional capillary density (96) as described in sections III*B*, X, and XI*C*. Thus, under the conditions of such studies, the suffusing solution may influence blood flow and oxygen gradients in the tissue. If the oxygen measurements are optical in nature, then the muscle may be covered with polyvinyl film or the tissue enclosed in a chamber and the suffusing solution discontinued.

B. Environment Isolated Preparations

Introduction of the window chamber technique provided an additional refinement since the tissue is allowed to recover from the acute effects of surgery for 2–4 days before study. The animal is studied in the unanesthetized state, and it develops its own "milieu interieur," independently of most conditions in the environment. This type of preparation was originally developed for studies using the rabbit ear (19, 103) and was implemented in rodents by Algire (1), but initially depended on the formation of scar tissue to fill the chamber. The model was modified by Reinhold (97), who implemented a skinfold window chamber in the rat where the window chamber supported and protected a thin layer of preexisting tissue in the dorsal region. This was one of the first models that allowed the long-term study of a preestablished microvascular system in subcutaneous connective tissue and skeletal muscle. The model was further elaborated by Papenfuss et al. (85) and was adapted by Endrich et al. (31) to the hamster, by Smith et al. (118) to the rat, and by Leunig et al. (73) to the mouse. A cranial window developed by Levasseur et al. (75) has similar features. These preparations allow the study of the tissue after the initial surgical trauma has subsided and in the conscious animal. The tissue is isolated from the environment, forms its own milieu interieur, and can be studied for periods as long as a week in the hamster according to our own experience and 1 mo in the rat as indicated by Smith et al. (118), before the tissue begins to exhibit features of scar tissue, including edema, increased tissue optical density (lower light transmission), and venules become tortuous.

IV. LONGITUDINAL GRADIENTS IN THE MICROCIRCULATION

It seems likely that some loss of oxygen from the blood begins as soon as the blood exits the lung. However, the amount of oxygen lost is apparently not significant until blood reaches the smallest arteries since the oxygen level in the large arterioles is very similar to that in these vessels (138). This loss of oxygen accelerates in the arteriolar network as documented by techniques that measure periarteriolar P_{O_2}, HbO_2 saturation, and intravascular P_{O_2}.

As described below, measurements of local P_{O_2} levels in the microcirculation have provided evidence that a longitudinal gradient is present to a greater or lesser degree in the arteriolar network of almost all vascular beds studied. It must be borne in mind that a variety of measurement techniques were employed and the actual values that were obtained may have reflected the vagaries of surgical preparation, level of anesthesia, and oxygen level of the suffusate, if used.

A. Periarteriolar Oxygen Determinations With the Microelectrode Technique

Duling and Berne (25) used Whalen-type polarographic microelectrodes (2- to 6-μm tip diameter, Ref. 141) and estimated blood P_{O_2} by placing the microelectrode on the external wall of the arterioles of the hamster cheek pouch preparation and the rat and hamster cremaster muscle. The P_{O_2} of arterioles of 60–100 μm diameter in the hamster cheek pouch was 35 ± 4 mmHg (67 ± 8% estimated HbO_2 saturation assuming intraluminal and periarteriolar P_{O_2} are the same) and fell to 24 ± 3 mmHg (44 ± 6% saturation) in terminal arterioles of 10–20 μm diameter, 20 ± 3 mmHg (33 ± 6% saturation) in arterial capillaries, and 8 ± 2 mmHg in the tissues, using a suffusion solution equilibrated at a P_{O_2} of 39 mmHg and when animals breathed room air. When the hamster was respired with 95% oxygen, the P_{O_2} values increased to a greater degree in the proximal vessels, being 152 ± 13 mmHg (100% saturation) in the 60- to 100-μm arterioles and 37 ± 9 mmHg (73 ± 18% saturation) in arterial capillaries. In the rat breathing room air, the longitudinal P_{O_2} gradient in cremaster muscle arterioles was also present, although absolute values were significantly higher in all vessels compared with the hamster cheek pouch, probably reflecting the higher P_{50} value for rat red blood cells compared with those of the hamster. In a subsequent study on the hamster cheek pouch, Duling (24) reported periarteriolar P_{O_2} values of 48 ± 2 mmHg in 30- to 50-μm arterioles, 39 ± 2 mmHg in 10- to 20-μm arterioles, 30 ± 3 mmHg in 7- to 12-μm arterioles, and 18 ± 2 mmHg in 4- to 6-μm arterioles.

Lash and Bohlen (72) observed a periarteriolar P_{O_2} longitudinal gradient in the resting rat spinotrapezius muscle where oxygen tension fell from 50 ± 12 mmHg (72 ± 17% estimated saturation) in first-order (A1) arterioles (41 μm mean diameter) to 46 ± 3 mmHg (61 ± 4% saturation) in second-order (A2) arterioles (28 μm mean diameter) and 31 ± 3 mmHg (40 ± 4% saturation) in third-order (A3) and fourth-order (A4) arterioles (11 to 7 μm mean diameter). They also examined the effect of

muscle contraction on the P_{O_2} at these sites. Somewhat surprisingly, during a 5-min period of 2- to 12-Hz electrical stimulation of the muscle, periarteriolar P_{O_2} initially fell but returned to control levels at all stimulation frequencies. Flow rose by as much as 150% above control during muscle contraction. Thus it appears that the increased flow counterbalanced the effect of increased tissue oxygen consumption on periarteriolar and tissue oxygen tension, and the longitudinal gradient was maintained.

Boegehold and Johnson (9) studied the exteriorized sartorius muscle of the cat suffused with a solution equilibrated with 95% N_2-5% CO_2 and obtained periarteriolar P_{O_2} values of 52 ± 3 mmHg adjacent to second-order arterioles and 40 ± 2 mmHg for fifth-order arterioles. During reduced blood flow with sympathetic nerve stimulation, the periarteriolar P_{O_2} values were 25 ± 4 mmHg in second-order arterioles and 20 ± 4 mmHg in fifth-order arterioles. Thus reducing blood flow dropped both the absolute values and the longitudinal gradient of periarteriolar P_{O_2} in the arteriolar network. Adding 10% oxygen to the suffusate solution did not change the periarteriolar P_{O_2} significantly due to arteriolar constriction and reduced blood oxygen delivery.

Duling et al. (26) measured the periarteriolar P_{O_2} distribution in the pial microvessels of the cat and found a systematic longitudinal decrease from 99 ± 11 mmHg (98 ± 1% saturation) in vessels of 230 μm diameter to 73 ± 4 mmHg (94 ± 2% saturation) in vessels of 22 μm diameter. In the pial vessels of the rat, Ivanov et al. (55) reported periarteriolar P_{O_2} values of 75 ± 3 mmHg (87 ± 2% saturation) in 35 μm arterioles and 43 ± 3 mmHg (78 ± 2% saturation) in 8–12 μm arterioles. Blood samples from the femoral artery averaged 95 mmHg (99% saturation). They estimated that 21% of the oxygen present in arterial blood is lost before the capillary network. In a later study on rat pial vessels, the periarteriolar P_{O_2} of first-order arterioles (45 ± 7 μm) was 81 ± 6 mmHg or 94 ± 2% HbO_2 saturation and fell to 76 ± 11 mmHg (93 ± 6% saturation) in third-order arterioles (26 ± 7 μm) and 62 ± 12 mmHg (84 ± 11% saturation) in fifth-order arterioles (8 ± 2 μm) (138). The systemic HbO_2 saturation averaged 95%. It is notable that a significant longitudinal gradient was found in arterioles of such a tissue, which is normally subjected to high flow conditions. When rats were respired with 100% oxygen the periarteriolar P_{O_2} values rose to 241 ± 27 (SE) mmHg in 30 μm arterioles and 154 ± 11 mmHg in 10 μm arterioles (56). Blood samples from the femoral artery averaged 345 ± 6 mmHg. All P_{O_2} values indicate 100% saturation. A significant longitudinal gradient of arteriolar P_{O_2} was also observed in retinal vessels of the cat where perivascular P_{O_2} of a 50 μm arteriole fell an estimated 2.4–3.8 mmHg over a distance of 500 μm (16).

It should be noted that in these measurements, no allowance or correction was made for the effect of the catchment volume of the microelectrode, which varies with tip size. As a result, the periarteriolar P_{O_2} measured with different size microelectrodes provides varying estimates of intravascular P_{O_2} depending on the relative position of the microelectrode tip and the blood tissue interface. This problem was in part resolved by the introduction of microvessel blood spectrophotometry.

B. Intravascular Oxygen Determinations With the Spectroscopic Technique

The spectroscopic technique for measuring blood P_{O_2} in the microvessels was developed and used by Pittman and Duling (90) to map oxygen distribution in the arteriolar network of the hamster cheek pouch and corroborated the findings based on microelectrode measurements. Similar studies were carried out in the hamster retractor muscle by Swain and Pittman (123), showing, in essence, that in connective tissue and muscle a significant amount of oxygen has left the circulation before blood arrives to the capillaries. These authors reported that while femoral artery saturation was 87%, first-order arterioles (60 μm) had a saturation of 71 ± 7% (43 mmHg estimated P_{O_2}) while fourth-order arterioles had a saturation of 60% (33 mmHg). These authors reported that oxygen saturation fell by ~2%/mm vessel length in the first-order arterioles and 18%/mm vessel length in fourth-order vessels. Kobayashi and Takizawa (66) reported an oxygen saturation of 98.6 ± 5.4% (90–160 mmHg) in 1A arterioles of the rat cremaster muscle(110 ± 22 μm) and a gradual reduction along the network to 64.2 ± 4.5% (44.2 mmHg) in the 4A arterioles (20 ± 4 μm) when the animal respired 30% oxygen in nitrogen. They also measured intravascular pH using a pH-sensitive dye, 1-hydroxypyrene-1,3,6,8-trisulfonic acid, which does not penetrate the cell membrane and found a significant reduction from 7.39 ± 0.02 in 1A arterioles to 7.26 ± 0.05 in 4A vessels. When breathing 12% O_2 in N_2, oxygen saturation fell from 47.0 ± 5.5% (36.6 mmHg) in 1A vessels to 25.1 ± 3.8% (23.0 mmHg) in 4A arterioles. The change in pH was considerably greater, falling from 7.36 ± 0.01 in 1A arterioles to 7.01 ± 0.06 in 4A vessels. This finding suggests that the Bohr effect may aid in unloading oxygen from red blood cells in the arteriolar network either due to CO_2 with normoxia as suggested by Pittman and Duling (91) or to lactic acid production during hypoxia.

Seiyama et al. (109) found a drop in O_2 saturation from 73 ± 8% upstream to 66 ± 8% downstream at two points averaging 73 ± 13 μm apart in 7–11 μm arterioles of the rat exocrine pancreas. The difference in O_2 saturation more than doubled with secretin administration, and red cell velocity also rose, indicating an increase in oxygen consumption of the acinar cells, assuming that vessel diameter did not decrease greatly at the same time causing a reduction of blood flow.

Bohlen and Lash (11) found that arteriolar saturation between 2A arterioles and the villus tip in the small intestine decreased by ~10% in rats and ~15% in rabbits. The oxygen loss in the inflow vessels was ~11.5% saturation/mm vessel length in rats and 7%/mm vessel length in rabbits. The fall in saturation occurred mainly in the terminal arterioles, but the authors noted that flow rates in the larger arterioles were very high. It would be expected that for arterioles of the same diameter, the fall in saturation would be less in arterioles with greater flow.

C. Cryoscopic Determination of Hemoglobin Saturation

Gayeski and Honig (36) used this method to determine the myoglobin and hemoglobin saturation in skeletal and cardiac muscle at various levels of activity. In dog gastrocnemius muscles that were electrically stimulated at 4 Hz, they found that oxyhemoglobin saturation was 88% in arterioles of 100 μm diameter and 86% in 40 μm diameter arterioles (48). Similarly, there was not a significant HbO_2 saturation gradient in the arteriolar network with reduced flow and with free flow during maximal exercise. In working dog heart, this group found that the oxyhemoglobin saturation was not significantly different for arterioles of 180 μm diameter (95%) and arterioles of 20 μm diameter (93%) (47).

D. Intravascular Oxygen Determinations by Phosphorescence Quenching

Studies in the awake hamster model (62) showed that the mean arteriolar P_{O_2} for first order (A1) arterioles was 52 ± 10 mmHg, a reduction of 19 mmHg from systemic arterial P_{O_2} (71 ± 11 mmHg). When vessels were grouped in orders according to the position in the network, a strong positive and significant correlation was found between internal arteriolar diameter and intravascular P_{O_2}. Information on the magnitude of the oxygen loss in individual arterioles of the hamster cheek pouch was reported by Torres Filho et al. (130), who found that the average decrease in P_{O_2} from first- to fourth-order arterioles was 18 mmHg (or 39% of saturation). While a significant P_{O_2} decrease was found in moving downstream between vessels of different orders, the longitudinal P_{O_2} gradient was small for a given arteriole, suggesting that the diffusion pattern at the bifurcations may be significantly altered by the geometry of the bifurcation and the increase in surface area. In 15 arterioles, intravascular P_{O_2} measurements were made sequentially at 70- to 600-μm intervals in the direction of blood flow. In most cases there was a decrease in P_{O_2}. Dividing each P_{O_2} difference by the distance between the measurement locations yielded an average P_{O_2} gradient for each arteriole, which was converted to percent of saturation according to the oxygen dissociation curve for hamster blood (134). The mean longitudinal saturation gradient (%/mm) obtained for the arteriolar network was 3.4 ± 0.4%/mm, or 3.0 ± 0.5 mmHg/mm. Fourth-order arteriolar P_{O_2} was 34 ± 2 mmHg.

Data on longitudinal gradients in the arteriolar network for a number of these studies are shown in Figure 1, *left*. As is evident from the preceding descriptions and Figure 1, there are substantial differences in the longitudinal gradients in different vascular beds; the gradient is much less in the brain compared with the hamster window preparation, for example. There also appear to be differences dependent on the measurement technique employed; the gradient was reported to be much less in resting skeletal muscle with the cryoscopic method than that reported with the microelectrode or phosphorescence techniques.

V. CAPILLARY LONGITUDINAL GRADIENTS

The longitudinal gradients in the capillary network vary greatly depending on the vascular bed studied. Duling and Berne (25) noted that when the hamster was breathing room air the perivascular P_{O_2} values measured with the microelectrode technique in the cheek pouch indicated that the blood was 67% desaturated upon entering the capillaries. Since venous blood P_{O_2} was reported to be higher (36 mmHg), we may hypothesize that in this tissue, capillary P_{O_2} represents the lowest intravascular P_{O_2} value. A study in the awake hamster model (62) using the phosphorescence technique similarly reported a small fall in P_{O_2} between terminal arterioles and venules, indicating an approximately constant capillary P_{O_2} of ~30 mmHg. Also, it was found in this preparation that fourth-order arteriolar P_{O_2} was 34 ± 2 mmHg and tissue P_{O_2} between the capillaries was 25 ± 6 mmHg, showing that tissue and capillary P_{O_2} is relatively uniform in this preparation. In the study of Torres Filho et al. (130), the change in O_2 saturation from A4 arterioles to venules was only 8%. These data show that in this unanesthetized hamster model the whole microvascular network participates in tissue oxygenation and that the capillaries do not play a major role in the process. In the studies of Pittman and Duling (90) on the hamster cheek pouch preparation, it was found that the mean change in blood saturation as blood traverses the capillaries was 9 ± 2%, a value which reduced to 5% when the contribution of each vessel was weighted according to flow rate. This correction was introduced to reduce the bias caused by the large change in oxygen saturation of slow flowing capillaries, which otherwise do not contribute significantly to the tissue oxygen delivery. In the intestinal muscle of rats, Bohlen (10) found that tissue P_{O_2} measured with a microelec-

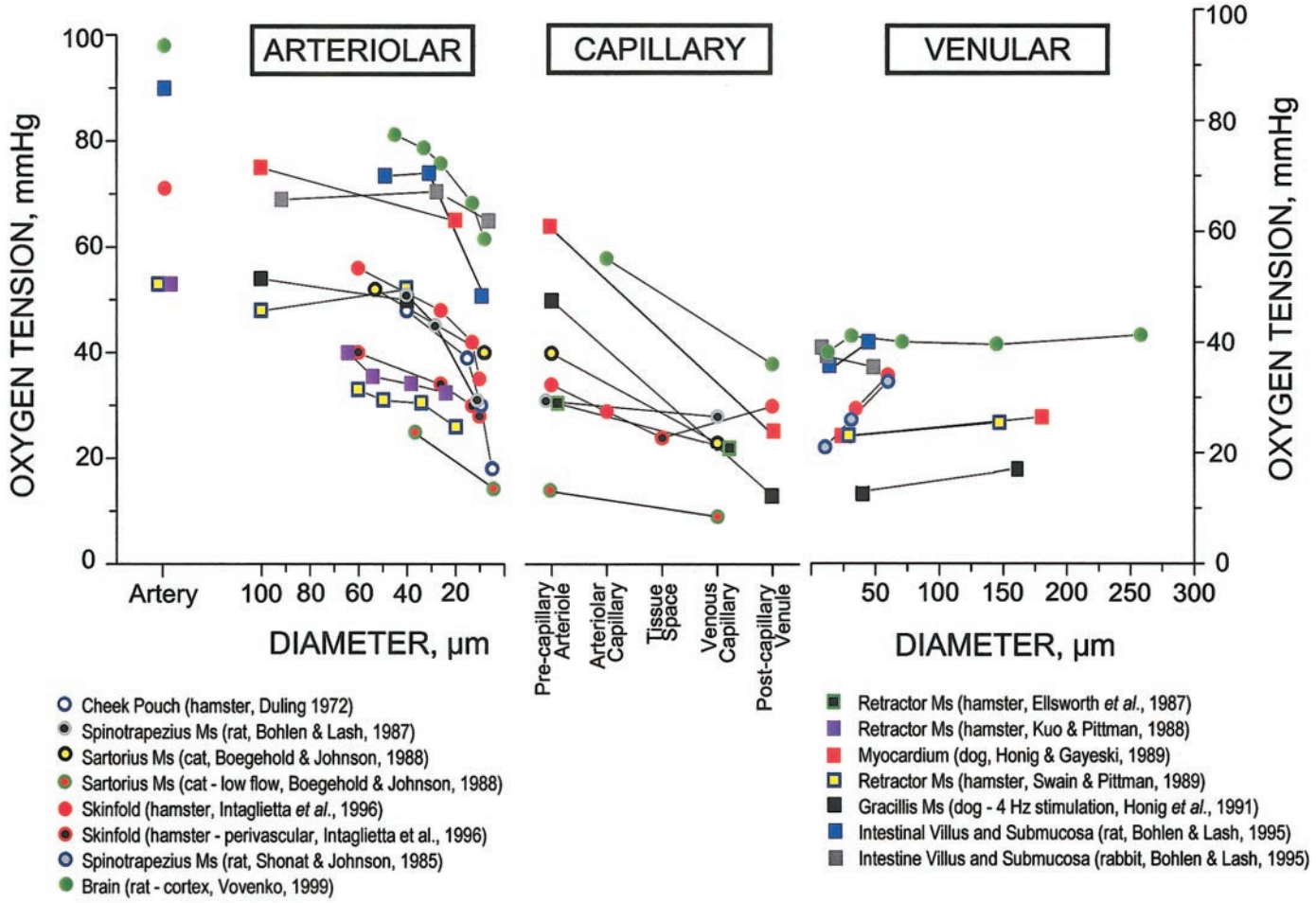

FIG. 1. Distribution of the oxygen tension in the microcirculation found in different tissues with different techniques. Microelectrode measurements: Cheek pouch, hamster (24); brain cortex, rabbit (138); sartorius muscle, cat (9); spinotrapezius muscle, rat (72). Microspectrophotometric technique: retractor muscle, hamster (29, 70, 123); intestinal villus and submucosa, rat (11); intestinal villus and submucosa, rabbit (11). Cryoscopic technique: myocardium, dog (47); gracilis muscle, dog (48). Phosphorescence quenching: skinfold preparation, hamster (51); spinotrapezius muscle, rat (113). Squares signify that the original measurement was in terms of hemoglobin oxygen saturation (%), and circles are measurements of oxygen partial pressure (mmHg). Oxygen saturation data were converted to oxygen partial pressures using animal specific oxygen dissociation curves [dog, rabbit (2); rat (125); hamster (90)].

trode at a point 15 μm from an adjacent capillary fell from 25 ± 1 (SE) mmHg near arterial capillaries to 22 ± 1 mmHg near venous capillaries. Lash and Bohlen (72), in the resting rat spinotrapezius muscle, reported levels of 31 ± 3 mmHg in third- and fourth-order arterioles (11 to 7 μm) and 28 ± 14 mmHg in tissue sites between capillaries at the midlength of these vessels. During a 5-min period of electrical stimulation of the muscle at 2–12 Hz, capillary and periarteriolar P_{O_2} initially fell and then fully recovered during the stimulation period at all stimulation frequencies except at 12 Hz. Somewhat larger reductions in P_{O_2} in the capillary region were found by other investigators. Boegehold and Johnson (9), using the microelectrode technique, found a drop from 40 ± 2 mmHg at periarteriolar sites for fifth-order arterioles to 23 ± 3 mmHg at tissue sites between venous capillaries in cat sartorius muscle. During reduced blood flow with sympathetic nerve stimulation, the P_{O_2} values were 20 ± 4 mmHg in fifth-order arterioles and 9 ± 2 mmHg at the tissue sites. Adding 10% oxygen to the suffusate solution did not change periarteriolar P_{O_2} but increased the tissue P_{O_2} to 34 ± 3 mmHg.

Ellsworth and co-workers (29, 20), using a two-wavelength spectrophotometric method to determine hemoglobin oxygen saturation, found that HbO_2 saturation in capillaries decreased from 61% at the arterial end to 40% at the venous end in hamster retractor muscle. Average capillary length was 412 μm. The rate of oxygen loss per unit capillary length calculated from these estimates (0.051% SO_2/μm) is about one-half that measured in short segments of arterial and venous capillaries, possibly due to oxygen transfer between adjacent capillaries. In a separate study, Ellsworth and Pittman (28) found that an arteriole crossing the capillary bed would significantly

reduce or even reverse this gradient locally while a venule crossing the bed would cause it to increase.

The largest fall in HbO_2 saturation across the capillary network was reported by Honig et al. (48), who used the cryoscopic technique. In that study, saturation fell from 86% to 14% between 20 μm arterioles and 20 μm venules of the dog gracilis muscle that was electrically stimulated at 4 Hz. Somewhat surprisingly, the findings were similar in this muscle at rest when blood flow was reduced to ~25% of that for free flow in resting muscle. Saturation fell from 93% in 20 μm arterioles to 38% in 20 μm venules of the dog heart, and from 86% to 45% in 20 μm arterioles to 20 μm venules of the rat heart (47). These findings are consistent with the very small drop in saturation in the arteriolar network found with this technique as described in section IV*C*.

In the brain the longitudinal capillary gradient appears to be substantial. In pial microvessels of the cat, Duling et al. (26) found that perivascular P_{O_2} was 73 ± 4 mmHg in 22 μm arterioles while tissue P_{O_2} was only 11 mmHg. Rubin and Bohlen (101) found that tissue P_{O_2} in the capillary bed of the cerebral cortex of the rat averaged 13 ± 1 mmHg (SE), but over 20% of the values fell below 5 mmHg while a few (5%) were 30 mmHg or higher. Ivanov et al. (55) reported that P_{O_2} dropped from 43 ± 3 mmHg in the terminal arterioles of the rat pia to 26 ± 3 mmHg in small venules, representing a fall of ~38% in blood oxygen content. Vovenko (138) found that perivascular P_{O_2} in the pial microcirculation of the rat was 58 ± 11 mmHg (82 ± 9% saturation) at the arterial end of capillaries and fell to 41 ± 11 mmHg (59 ± 18% saturation) at a site ~260 μm downstream in the capillaries and dropped further to 38 ± 12 mmHg (54 ± 18% saturation) in fifth-order venules (13 ± 6 μm diameter). In this case the rate of oxygen loss was 0.16% SO_2/μm, or about three times greater than seen in hamster retractor muscle at rest across the full capillary network. This difference is not unexpected, considering the higher metabolic rate of the brain (3.5×10^{-2} ml $O_2 \cdot min^{-1} \cdot g^{-1}$, Ref. 3) compared with resting skeletal muscle (4.4×10^{-3} ml $O_2 \cdot min^{-1} \cdot g^{-1}$, Ref. 87).

Bohlen and Lash (11) found that HbO_2 saturation in the intestinal mucosa decreased by 5% along the small arterioles and villus capillaries in the intestine of the rat and by 15% in rabbits. In both species, 70–90% of the total oxygen loss in the intestinal mucosa occurred in the small arteriole and capillary region.

Seiyama et al. (109) found in hepatic sinusoids of the rat (which are supplied from both the hepatic artery and portal vein) the HbO_2 saturation decreased from 39 ± 9 to 26 ± 8% over a 70 μm distance with normal systemic hematocrit or 0.19% SO_2/μm, a rate of oxygen loss similar to that seen in the brain. The difference in saturation between upstream and downstream sites almost doubled with moderate anemia, although volume flow did not change, perhaps reflecting in part the reduced oxygen content of the blood.

It has been pointed out by several investigators that the oxygen transport process from blood to tissue at the capillary level may be significantly impeded by the presence of plasma gaps between red blood cells (33, 43). In this regard, it is of interest that Zheng et al. (147) utilized the phosphorescence signal from the plasma in the hamster retractor muscle capillary to estimate a P_{O_2} gradient of ~4 mmHg/μm in the plasma gap between red blood cells. This comparatively large gradient suggests that one of the limitations to complete extraction of oxygen from the red blood cell in exercising muscle is the diffusional resistance in the capillaries (122, 139), a limitation that may be further augmented by the P_{O_2} gradient between the red blood cell and the plasma.

The Fåhraeus effect may be another factor that significantly influences the longitudinal gradient in the arterioles, although this possibility has not been emphasized in the literature, which focuses on how this phenomenon influences the fluid dynamics of the microcirculation (39). The reduction of hematocrit in small-diameter blood vessels and the formation of a plasma layer lowers the intrinsic oxygen-carrying capacity of blood in the arterioles, which increases the fall in oxygen content in these vessels as oxygen diffuses out. Conversely, as discussed by Hellums (43) and Hellums et al. (44), the formation of a plasma layer constitutes an additional barrier to the outward diffusion of oxygen, in part offsetting the effect of lowered hematocrit on the longitudinal gradient.

Data on longitudinal gradients in the capillary network for a number of these studies are shown in Figure 1, *middle*. As noted for the longitudinal gradients in the arteriolar network, there are differences that appear to be related to the specific vascular bed (brain vs. hamster window preparation) and to the technique employed (cryoscopic method vs. microelectrode and phosphorescence techniques).

VI. VENULAR LONGITUDINAL GRADIENTS

Pittman and Duling (90) found that larger venules in the hamster cheek pouch preparation had greater mean saturation than small venules. In the studies of Kerger et al. (62), in the awake hamster skinfold window preparation using the phosphorescence technique, venular capillaries and venules had respective P_{O_2} values of 30 ± 9 and 35 ± 10 mmHg.

Shonat and Johnson (113) studied the oxygen tension in the venous microcirculation of the rat spinotrapezius muscle utilizing the phosphorescence decay technique. They found that the mean intravascular P_{O_2} levels in postcapillary venules (diameter: 11 ± 4 μm), venular vessels (diameter: 31 ± 9 μm), and arcading venules

(diameter: 60 ± 22 μm) rose sequentially from 22 ± 9 to 26 ± 10 to 33 ± 8 mmHg, respectively, thus corroborating the presence of an increasing mean oxygen level in progressing downstream in this venular microcirculation.

Swain and Pittman (123) also found higher mean blood oxygen saturations levels in the 147 μm I.D. first-order vessels in the venular network of the hamster retractor muscle compared with 28 μm fourth-order vessels. These investigators found that blood oxygen saturation was distributed in such a fashion that vessels with high saturation had high flow rates and vice versa. To obtain the average values for the oxygen saturation in each branching order flow they weighted each saturation measurement, i.e., multiplied each saturation measurement by the corresponding flow rate and divided by the sum of all flow rates measured, with the effect that a vessels with low saturation and flow had little effect on the calculated average saturation for a given vessel order. Thus mean P_{O_2} values at upstream and downstream sites alone may not provide sufficient information to draw conclusions regarding the gain or loss of oxygen in the venular network. Regarding the mechanism behind the increase of blood P_{O_2} in the large venules seen in some tissues, Stein et al. found that mean P_{O_2} and oxygen saturation were both significantly higher in large (first-order) venules compared with end-capillary values in the hamster retractor muscle when breathing 30 or 21% O_2 but not when breathing 10% O_2. They suggested that a diffusional shunt from arterioles to venules at the level of first- and/or second-order arterioles when breathing 30 or 21% O_2 was responsible for the elevated oxygen levels in the large venules. In special circumstances, direct evidence of countercurrent exchange between arterioles and venules has been obtained as in the retinal circulation where the venous blood oxygen level rises as the two vessels travel side by side (16). This situation is somewhat unique since the vitreous humor adjacent to the venule of the eye does not consume oxygen and thus may allow countercurrent exchange to be manifest. There is no significant oxygen exchange between parallel arterioles and venules in the intestinal villus of the rat and rabbit perhaps because of the 300- to 500-μm separation and the oxygen consumption of the intervening tissue (11). In the submucosa of the rat and rabbit there is a fall (although modest) in oxygen saturation as the blood flows through the venular network. In the rat, this finding could reflect mixing of blood with higher saturation from the intestinal muscle with blood of lower saturation from the villi, but this explanation would not apply to the rabbit where the saturation in second-order venules is less than that from the villi and third-order venules of the intestinal muscle.

Gayeski and Honig (37) found a slight increase in mean HbO_2 saturation from 38 to 44% between venules of 25 and 180 μm in the dog heart and no apparent change in saturation between 20 and 160 μm venules of the rat heart using the cryoscopic technique. Also, in the working dog gracilis muscle (4 Hz electrical stimulation), there was a slight rise from 14 to 20% saturation between venules of 20 and 140 μm (48). Saturations varied widely among the small venules in these studies.

Vovenko (138) found in the venular network of the brain that P_{O_2} levels were very heterogeneous at each branching order, varying by as much as 60 mmHg. In the large venules intraluminal P_{O_2} measurements showed distinct flow streams from different tributaries with different oxygen levels, suggesting that the oxygen extraction from the deeper regions of the brain may be greater than those near the surface. Average values of P_{O_2} rose slightly from 38 ± 12 mmHg (54 ± 18% saturation) in 13 ± 6 μm fifth-order venules to 40 ± 9 mmHg (57 ± 18% saturation) in 71 ± 24 μm third-order venules, and 41 ± 10 mmHg (59 ± 14% saturation) in 258 ± 31 μm first-order venules. Despite the slight rise in average P_{O_2} apparent in the data presented above, venules of 10–40 μm diameter appear to supply oxygen to surrounding tissue as discussed in the section VIII. It may be speculated that the higher levels of oxygen in the larger venules and veins, whatever the mechanism, may serve a functional purpose. In contrast to the small collecting venules, the latter contain significant quantities of vascular smooth muscle (98) and may require a greater supply of oxygen for the oxidative metabolism of this tissue.

Data on longitudinal gradients in the venular network for a number of these studies are shown in Figure 1, *right*. Notable in this graph is the gradual rise in P_{O_2} for most vascular beds except for the venular networks of the hamster skinfold and rat spinotrapezius muscle where there is a substantial rise and the rabbit muscosa where there is a slight fall.

VII. INTERACTION OF ARTERIOLAR AND VENULAR GRADIENTS

The parallel arrangement of arterioles and venules has been shown to be present in several tissues (65), and functional studies of this configuration have shown that O_2 and CO_2 are transferred by diffusion between these vessels (28, 58, 100). In this situation the back diffusion of CO_2 into the arterioles decreases pH in these vessels causing the right shift of the oxygen dissociation curve by the Bohr effect. This was investigated by Kobayashi and Takizawa (66) (see sect. IV*B*) who found in rat cremaster muscle a pronounced decrease in pH with 12% O_2 in inspired gas from fourth-order arterioles to second-order venules, namely, the vessels that do not present the parallel configuration necessary for countercurrent exchange. This study showed that in hyperoxia (30% O_2) shunting contributes to the stabilization of tissue P_{O_2} protecting the tissue from excessive P_{O_2}. Conversely, in

hypoxia, CO_2 shunting lowers arteriolar blood pH facilitating the release of oxygen from blood. It should be noted that the lowering of pH in blood as it transits from the arteriolar to the venular portion of the microvascular network allows more oxygen to be delivered with comparatively small changes in blood P_{O_2} (140).

VIII. LONGITUDINAL GRADIENTS: SUMMARY

1) In vascular beds with low flow per gram tissue and low metabolic demand such as resting skeletal muscle, there is a significant longitudinal gradient of P_{O_2} and oxyhemoglobin saturation in the arteriolar circulation. Conversely, the gradient is much less in tissues with higher blood flow per gram tissue and metabolic demand such as brain and intestine. The variations could reflect differences in the ratio of volume flow of blood to vascular area available for exchange in the arteriolar network. An additional factor is the state of constriction of the arterioles, which would be higher in resting muscle. As discussed in section x*E*, there is evidence that the arteriolar wall consumes an extraordinary amount of oxygen, and this consumption may be greater when vascular tone is increased (51). It is of interest that when contraction was induced in a microcirculatory preparation (spinotrapezius muscle) the longitudinal gradient changed only transiently (72). In this instance it is possible that increased oxygen demand of the parenchymal cells is offset to a degree by the reduction in oxygen demand of the smooth muscle cells in the dilated arteriole. Finally, the absence of a significant longitudinal gradient in contracting muscle as assessed by the cryoscopic method (48) is consistent with the findings in tissues with a high metabolic rate, but its absence in resting muscle with greatly reduced flow does not agree with findings obtained with in vivo microelectrode, phosphorescence, or hemoglobin saturation methods.

2) Consistent with the findings cited previously in the arteriolar network, the contribution of capillaries to the exchange process for oxygen as assessed from the longitudinal gradient also varies greatly among vascular beds, being lowest for resting skeletal muscle and highest for rapidly metabolizing tissues such as brain and myocardium.

3) Mean values for venular/venous P_{O_2} in certain tissues are higher than capillary and tissue P_{O_2}, but the interpretation of these findings is complicated to a degree by the fact that flow in this region of the circulation is quite heterogeneous. These observations suggest that in these tissues microvascular arteriovenous shunts (32) of an anatomic or functional nature transport oxygenated blood into the venous microcirculation. The Bohr effect may significantly enhance countercurrent exchange between arteriolar and venular networks in certain vascular beds.

4) The terminal arteriole/collecting venule oxygen content difference in tissues with low metabolic rate is considerably smaller than or in some cases similar to the drop in oxygen saturation from arterial blood to the terminal arterioles.

IX. RADIAL GRADIENTS

Information on radial gradients of oxygen across the vascular and parenchymal tissue, in the region defined by the blood tissue interface and onward into the tissue, is considerably more limited than that described above for longitudinal gradients in the microcirculatory vessels which were often obtained incidental to other studies. Several studies have focused on P_{O_2} gradients across the vascular wall, while several others determined the radial gradient in the surrounding tissues.

A. Arterial Wall Radial Gradients

Gradients have been determined in the wall of normal and diseased dog and rabbit carotid arteries in vivo with the oxygen microelectrode technique (105, 116). These studies demonstrated a shallow P_{O_2} gradient as the electrode tip penetrated through the smooth muscle layer from the abluminal surface of the vessel and a sharp rise in P_{O_2} of ~40 mmHg or more as the electrode tip was moved from a site 99% of the distance through the wall into the lumen of the blood vessel as shown in Figure 2. This steep P_{O_2} gradient at the inner surface of the vessel was a consistent observation in a variety of studies (84, 104, 105).

B. Arteriolar Radial Gradients

Duling and Berne (25) reported that the measured P_{O_2} rose only 1 or 2 mmHg after advancing the electrode tip into the arteriolar lumen of the hamster cheek pouch. Radial gradients in the periphery of arteriolar microvessels were first observed by Duling et al. (26), who by means of microelectrode measurements determined that in the pial microvessels they were of the order of 1 mmHg/μm of diffusion path. Later studies by Ivanov et al. (56) and Vovenko (138) in the pial circulation with the microelectrode technique showed a decline of the gradient from ~1.5 mmHg/μm of diffusion path in the immediate vicinity of the wall to ~0.5 mmHg/μm at a site 40 μm distant. In the vitreous humor of the eye (which does not consume oxygen), the periarteriolar gradient is much lower, being of the order of 0.1 mmHg/μm in the region 10–30 μm from the wall of an arteriole ~75 μm in diameter (16).

Lash and Bohlen (72) measured perimicrovascular

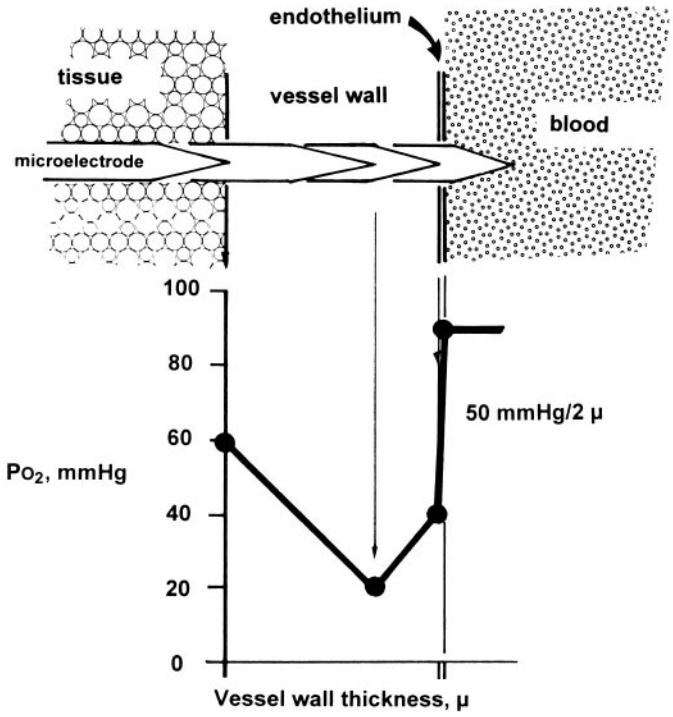

FIG. 2. Profile of P_{O_2} in the vessel wall of the rabbit aorta determined by Santilli et al. (105), by advancing a microelectrode from the abluminal side into the vessel wall. These vessels are devoid of vasa vasora, thus the P_{O_2} gradients are due to diffusion from the blood and tissue compartments and oxygen consumption. Because the endothelium is not a barrier to oxygen diffusion, and there is no specific resistance to diffusion at the blood-tissue interface, the steep gradient noted as the microelectrode transverses the last 2 μm of the vessel wall must be due to oxygen consumption in the endothelium. This gradient is of the order of 20 mmHg/μm.

and tissue P_{O_2} in the rat spinotrapezius model with 6- to 8-μm-diameter microelectrodes. They found a progressive fall in P_{O_2} along the arteriolar network but only a small difference between distal arterioles and capillaries. The periarteriolar average P_{O_2} in A3 to A4 arterioles was 30 mmHg, while pericapillary P_{O_2} was 28 mmHg, which was lower than perivenular P_{O_2}. Thus if we compare these data with other reported oxygen distributions in the arteriolar microcirculation, it would appear that there must be a substantial gradient of P_{O_2} near the arterioles, since their perivascular P_{O_2} is similar to that of capillaries.

Radial gradients have also been determined across the vascular wall in the arteriolar network of human tumor implanted in SCID mice in awake conditions (128) and the arterioles of the hamster window preparation (51) and the rat cremaster muscle preparation (112) using the phosphorescence technique. Intaglietta and co-workers (51) have measured the P_{O_2} in the blood at the vessel wall and just outside the vessel in the surrounding tissue. The radial P_{O_2} differences are shown in Figure 3 for these vessels. In this instance there is a steep gradient across the arteriolar wall, typically of the order of 18 mmHg in the A1 arterioles of this vascular bed and diminishing in the more distal vessels. Results obtained by Shibata et al. (112) in a rat skeletal muscle preparation were proportionally similar to the wall gradients found in the hamster window model, namely, 45 ± 10 mmHg in 80- to 120-μm-diameter arterioles to 14 mmHg in A3 arterioles (diameter range indicated to be <60 μm and estimated to be ~30 μm). These investigators utilized a system built according to the guidelines of Torres and Intaglietta (129), using minimal light exposure, and averaged repeated phosphorescence decay curves from repeated flashes. Tsai et al. (132) reported a P_{O_2} ranging from 27 to 14 mmHg across the arteriolar wall of rat mesentery, depending on blood P_{O_2} (59 to 23 mmHg), yielding a gradient in the range of 11 to 4 mmHg/μm across the vessel wall and a gradient of ~0.7 mmHg/μm in a surrounding 40-μm tissue region. Thus several studies have reported a very steep gradient of 10 mmHg/μm or more in the arteriolar wall while the gradient in the surrounding parenchymal tissue is generally of the order of 1 mmHg/μm. The implications of this observation are considered further in sections XI and XII.

C. Capillary Radial Gradients

Vovenko (138) reported radial gradients of ~0.25–0.5 mmHg/μm in a 40-μm region immediately adjacent to capillaries in the rat pial microcirculation using the microelectrode method. These data suggest an overall difference of 10–20 mmHg between capillary blood and the distal sites in the tissue supplied by the capillary. Using the cryoscopic technique and myoglobin saturation data, Gayeski and Honig (36) estimated gradients of 0.02–0.10 mmHg/μm near the sarcolemma of myocytes in maximally exercising red muscle and much lower gradients in

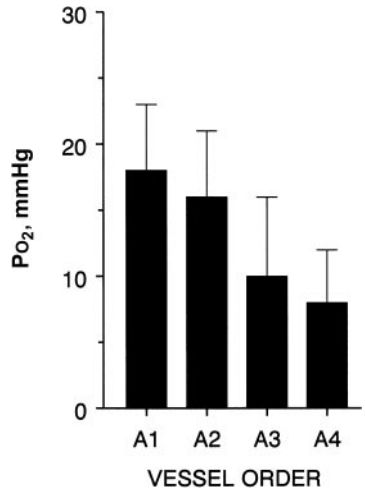

FIG. 3. P_{O_2} difference across the arteriolar wall for four orders of arterioles with the following diameters (in μm, means ± SD): A1, 85.1 ± 23.1; A2, 28.4 ± 11.7; A3, 9.8 ± 3.2; A4, 6.4 ± 2.1. [Data from Intaglietta et al. (51).]

the cell interior. The data of Intaglietta et al. (51), using the phosphorescence method, indicate that the gradient in the tissue in the immediate vicinity of the capillaries is of the order of 1.5 mmHg/μm. Wittenberg and Wittenberg (144) calculated the gradient in skeletal muscle consuming oxygen at the maximal sustainable steady-state rate to be 10–20 mmHg/μm. Because this rate is ~10 times the consumption at rest, this value corresponds to 1–2 mmHg/μm for skeletal muscle at rest. Within the capillary, the radial distance from the red blood cell to the wall would be influenced by factors such as the axial migration of red blood cells (the Fåhraeus effect) and the presence of a glycocalyx layer at the capillary wall (39).

D. Venular Radial Gradients

Richmond et al. (99) found a difference of 3.0 ± 0.6 mmHg between P_{O_2} in 20-μm collecting venules and tissue sites 30 μm distant in the rat spinotrapezius muscle using the phosphorescence technique. In all but 2 of 17 measurements the difference was significant. This difference increased to ~5 mmHg during 1 min of blood flow stoppage. These studies did not determine the possible contribution of the vessel wall to this gradient. Intaglietta et al. (51) determined that a wall gradient was present in the venules of the hamster window preparation, being of the order of 3 mmHg/μm. Using microelectrodes, Vovenko (138) found radial gradients of ~0.1–0.4 mmHg/μm in a 40-μm tissue region immediately adjacent to 10- to 40-μm venules of the rat pial microcirculation. These findings indicate that the venules can supply oxygen to the surrounding tissue, but the amount may vary with the particular vascular bed. As noted above, flow-weighted determination of change in HbO_2 saturation in venules of hamster cremaster muscle (123) indicated no net loss of oxygen in that venular network. In the microcirculation of eye, the situation is often reversed from that described above, with the venule gaining oxygen from the adjacent, nonmetabolizing vitreous humor in 5 of 13 cases (16).

There is generally a lack of detailed information on both longitudinal and radial gradients in any one vascular bed. An exception to this is the definitive report on the longitudinal and radial gradient for oxygen in the hamster window preparation presented by Intaglietta et al. (51). This paper used bar graphs to show the distribution of P_{O_2} as a function vessel order, a display that gives an intuitive understanding of the underlying processes. Figure 4 is a reproduction of these data, showing the oxygen level at each order of branching and how each level of branching unloads oxygen from the circulation. The data shown are typical for skeletal muscle preparations at rest and illustrate the substantial longitudinal and radial gradients in the arteriolar network of this vascular bed, the small

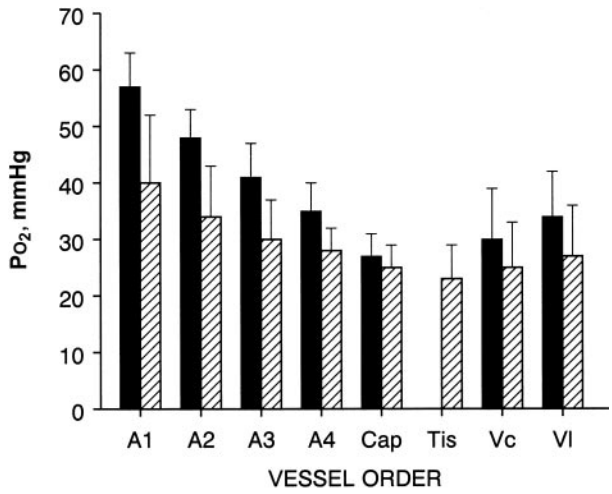

FIG. 4. Distribution of oxygen in the microcirculation of hamster skinfold preparation. Intravascular values are shown as solid bars, and extravascular values immediately outside the wall are shown as hatched bars. The vessel diameters for each order of branching are as follows (in μm, means ± SD): A1, 85.1 ± 23.1; A2, 28.4 ± 11.7; A3, 9.8 ± 3.2; A4, 6.4 ± 2.1; Vc, 21.0 ± 5.9; Vl, 88.7 ± 34.5. A1 through A4, arteriolar orders; cap, capillary; tis, tissue; Vc, collecting venule; Vl, large venule. [Data from Intaglietta et al. (51).]

amount of oxygen loss from the capillary network, and the increase in mean oxygen level in the venular network.

The delivery of oxygen to the tissue takes place through a system of conduits that sheds oxygen as blood transits to the peripheral circulation by the process of diffusion. The rate at which oxygen exits vessels and microvessels is determined by its diffusion constant in the tissue, which is approximately the same for blood and the soft tissues of the organism; thus there is no specific barrier to the exit of oxygen. As a consequence of this, the location of oxygen delivery depends also on the velocity with which blood transits, much in the same way as water can be transported with a leaky container if this moves rapidly. This combination of transport process results in a longitudinal gradient due to the progressive diminution of oxygen in the arteriolar network due to the diffusion process driven by the radial gradients. The radial gradient at its turn is a function of the amount of oxygen that the bloodstream brings at a given location and the oxygen consumption in the issue. Therefore, blood flow velocity and the longitudinal and radial gradients are intertwined, are relatively steady in normal basal conditions, and are characteristic of each tissue and organ.

As shown by the data in Figure 1, the delivery of oxygen does not necessarily occur predominantly in the capillaries, and in some tissues, delivery of oxygen by the arterioles is equally significant. In most tissues delivery of oxygen by the arterioles should in principle expose the tissue to significantly higher oxygen tensions than delivery of oxygen by the capillary system. Data on radial oxygen gradients provide evidence however of a steep

gradient around the arterioles; thus most tissue areas are not directly exposed to the high P_{O_2} in the arteriolar lumen. These considerations indicate that although a considerable amount of oxygen exits the arteriolar lumen, not all of this material reaches the parenchymal tissue, a phenomenon that appears to be related to the high oxygen consumption of the arterioles as discussed section XI. At the same time, it appears that a substantial part of the oxygen supply of the parenchyma in some organs is provided by the arterioles. This relieves the capillaries from their role of sole suppliers of oxygen to the tissue. The difference in P_{O_2} between precapillary arterioles and the venous capillaries or postcapillary venules is quite small in some tissues (Fig. 1). Furthermore, as shown in Figure 4, when the oxygen gradient in the immediate vicinity of the capillaries is subtracted from the intracapillary P_{O_2} value, we find that in some tissues the difference in P_{O_2} between capillaries and tissue is virtually nonexistent, indicating that in these organs the tissue is not oxygenated by the capillaries to a significant degree. Thus this vast network that permeates these tissues may well have other functions that may be more directly related to the metabolism and biochemical activity of the capillary endothelium. This is discussed in section XII*C*. In summary, the analysis of longitudinal and radial gradients suggests the existence of an oxygen sink at the arteriolar wall and capillary functions different from that of tissue oxygenation alone. The significant arteriolar wall oxygen consumption is a mechanism that competes with the process of tissue oxygenation by these vessels and in principle partially restores the capillaries to their role of oxygen suppliers to the tissue; however, as previously noted, the magnitude of this supply is at its turn dependent on the magnitude of the capillary endothelium oxygen consumption.

E. Radial Gradients: Summary

Comparing radial gradients in the three segments of the microvascular network shows, as expected, that the gradient is steepest in the arteriolar network and diminishes in the capillary and venular regions. While the gradients from these areas are also, as expected, steepest in the immediate vicinity of the vasculature, arteriolar vessels of rat mesentery and hamster window preparation show a pronounced drop across the vessel wall which, as discussed below, does not appear to be explained on the basis of diffusion alone. The cryoscopic method indicates a very shallow gradient at the sarcolemma and no significant difference in myoglobin saturation in the interior of the myocytes of maximally exercising gracilis muscle of the dog. In contrast, the microelectrode technique shows a substantial gradient in the brain tissue of the rat. The difference could reflect the effect of facilitated diffusion due to myoglobin (36) or differences in methodology. Unfortunately, the amount of data available on radial gradients in the vicinity of capillary networks is too limited to determine the cause of such striking differences. Available data indicate that there is a loss of oxygen from the venules. However, the radial gradients in the vicinity of these vessels are generally lower than in the other segments of the microcirculation when compared in the same tissue using similar methods as was the case with the findings cited above in the brain using the microelectrode technique. There is also a significant gradient across the venular wall in the hamster skinfold as shown in Figure 4. Despite this apparent loss of oxygen, the mean values quite consistently are higher in the larger venules. This may be due in part to flow streams with high volume flow and high oxygen levels mixing with low volume flow streams and low oxygen levels. However, other factors may also contribute. In some circumstances, uptake of oxygen into the venules from adjacent arterioles and surrounding tissue can occur as in the microcirculation of the eye. In other vascular beds there is evidence that oxygen diffusing from the arterioles may reach the more distal venules. These possibilities require further study.

X. METHODOLOGICAL EFFECTS ON MEASUREMENTS OF GRADIENTS IN THE MICROCIRCULATION

The data presented in the previous sections on longitudinal and radial gradients were obtained by a variety of methods in a number of different tissue preparations. To provide perspective on these measurements and the possible limitations in interpreting the findings, we provide here a consideration of specific characteristics of the various methods employed that appear to be relevant.

A. Measurement Techniques

Duling and Berne (25) measured the oxygen tension of arterioles of the rat and hamster cremaster muscle by placing the microelectrodes "... at the midpoint of the microvessels, in the vertical plane with the microelectrode just indenting the vessel wall." This description indicates that the sampling volume would include the vessel wall and a region of the flow stream, depending on the exact diameter of the electrode tip. Duling and Berne (25) also reported that the measured P_{O_2} rose only 1 or 2 mmHg after advancing the electrode tip into the vessel lumen. Also, Steenbergen et al. (119) found that periarteriolar P_{O_2} was virtually identical to the value estimated from the intravascular oxygen saturation and the oxygen saturation curve. To interpret these findings we must consider the role played by the catchment volume of the electrode. According to Kessler et al. (63), the minimum

catchment volume of an electrode is a hemisphere whose radius is 1.66 times the diameter of the electrode; thus the signal produced by the electrode is the integral of the oxygen sources within the described hemisphere. Duling and Berne (25) and Steenberger et al. (119) used electrodes whose average diameter was ~4 μm; therefore, those electrodes yield data that average the oxygen sources in a hemisphere of radius 6.7 μm from the surface of the electrode. If we suppose that the electrode tip was placed at ~2 μm from the blood/tissue interface (a location that may be in the tissue or in the vessels wall depending on the size of the arteriole), the electrode signal included data from a spherical segment in the bloodstream whose volume was ~40% of the total catchment volume. Considering the very high oxygen availability in blood relative to tissue (about a factor of 20 times), it would appear that such a measurement would primarily reflect the partial pressure of oxygen in blood, and further advancing the electrode toward the blood/tissue interface would not yield any appreciable change in the electrode signal, as found in both studies. These problems may be significantly less pronounced when electrodes recessed as indicated in section II*A1*; however, they cannot be excluded unless the recession length to electrode diameter ratio is specifically known for each electrode measurement.

Consequently, microelectrodes >2 μm tip diameter would not yield reliable measurements of oxygen distribution in the presence of steep and nonuniform oxygen gradients such as those in the vicinity of microvessels, and this technique when used to determine the periarteriolar P_{O_2} yields measurements that being close to those of luminal oxygen tension are therefore substantially higher than the value in the periarteriolar space.

As a corollary, microelectrode studies of oxygen distribution in the neighborhood of the blood vessel interface in general do not agree with the phosphorescence studies. In the neighborhood of the blood/tissue interface, the catchment volume of the electrode tip can include the flowing blood that is an oxygen source of very low source impedance and that is nearly uniform up to the blood/tissue interface. In other words, as the electrode tip nears the blood/tissue interface, the catchment volume is partially in the tissue and partially in blood, where the latter has a high oxygen concentration and therefore supplies oxygen into the catchment volume at much higher rate than when semi-hemispherical catchment volume is wholly immersed in the tissue, since flowing blood resupplies the consumed oxygen. The net effect of this process is that microelectrodes placed on the microvascular wall may overestimate the local partial pressure of oxygen and underestimate the radial gradients near the blood/tissue interface. An example of the effect of electrode tip diameter in the evaluation of vessel wall gradients is the difference in oxygen profiles in the arterial wall found by the studies of Santilli et al. (105), who used sharp metal electrodes of 1–2 μm diameter and consistently obtained a gradient of ~20 mmHg/μm across the endothelium of the aorta of the rabbit, vs. Buerk and Goldstick (14), who investigated various arterial blood vessels, including the rabbit abdominal aorta and obtained the value of 1.2 mmHg/μm aortic strips in vitro, with 5-μm tip diameter electrodes, and 0. 43 mmHg/μm in vivo in the dog thoracic aorta. It is notable that these contrasting results were found even though Santilli et al. used metal electrodes that typically have a greater catchment volume than the recessed electrode used by Buerk and Goldstick which points out the significance of the electrode tip diameter in these measurements.

In contrast, phosphorescence studies are minimally influenced by the light from adjacent regions because the area being measured is in focus and sharply outlined by the measuring slit, which can be directly observed visually superposed on the anatomical image under study. Under these conditions, signal contamination from lateral regions, particularly the bloodstream, is minimal or nonexistent. The possibility exists that signals may be integrated along the optical axis, thus averaging into the signal measurements from the tissue with lower P_{O_2}. The effect of this is that P_{O_2} measurements near the blood/tissue interface would be artificially lower than those corresponding to a given radial location in the interstitium. To analyze this effect, Tsai et al.(132) measured the oxygen profile in the tissue of the rat mesentery where the tissue was sandwiched between the lower glass pedestal and an upper film of Saran. This configuration causes a nearly uniform vertical (along the light path) distribution of oxygen tension at each potion in the outward direction. In this study the gradient across the vessel wall was found to be in the range of 10.8–5.6 mmHg/μm depending on blood P_{O_2}, which compares with studies of Intaglietta et al. (51) and Shibata et al. (112), who reported values in the range of 7.2–3.3 mmHg/μm in three-dimensional tissue. Given that the measurements in three-dimensional tissue should yield higher gradient values, rather than lower, it would appear that the problem of light emission integration does not significantly contribute to the signals obtained by phosphorescence (see Fig. 6).

The P_{O_2} value obtained by the phosphorescence technique could be influenced by oxygen consumption. This might not pose a problem in the flowing bloodstream where the oxygen supply is continuously replenished but could influence the measured P_{O_2} value in tissue fluid. This importance of this effect depends on the intensity of the flash as was shown in a study by Buerk et al. (17), who measured tissue P_{O_2} with an oxygen microelectrode while obtaining oxygen tension at the same site with the phosphorescence technique. The measured P_{O_2} value of the microelectrode was not affected during the flashing procedure, which employed a series of 100 weaker flashes

that were integrated to obtain a suitable signal-to-noise ratio. This comparison provides direct evidence for a negligible drop in oxygen level of the tissue using low-intensity repeated flashes and averaging the phosphorescence decay time from individual flashes. Thus it appears that the impact of the phosphorescence measurement on the P_{O_2} level can be mitigated by using lower intensity multiple flashes that allow sufficient time for oxygen to diffuse into the site of measurement.

Techniques utilizing the intensity of the emission of phosphorescent dyes modulated by the local tissue P_{O_2} have shown overall distributions of P_{O_2} in the tissue; however, they do not have the sufficient resolution to evidence P_{O_2} gradients across the vessel wall (54, 145).

B. Experimental Conditions of Tissues Investigated

Data obtained on oxygen gradients in vascular beds may also vary due to the experimental conditions imposed by the investigator. The level of anesthesia and particular anesthetic employed will influence the level of vascular tone as well as the responsiveness of the microvessels to vasoconstrictor and vasodilator stimuli (4, 21, 57, 71, 74, 77, 107). This in turn may influence the specific intravascular P_{O_2} distribution obtained during the experiment (60).

The oxygen gradients in vivo as reported here appear to be reproducible in a given vascular bed under specified conditions in a given laboratory. The preparations studied apparently had some degree of vascular tone (although this issue was not always examined). There is evidence that the normal regulatory mechanisms operate in such a manner as to set the oxygen levels in the microcirculation within a certain range. If the oxygen level of a suffusing solution over a microcirculatory preparation is increased, for example, the microvasculature responds in such a manner as to maintain the levels constant. This effect was first described by Duling (24), who showed with the microelectrode technique that the perivascular P_{O_2} at four levels of the arteriolar network and tissue P_{O_2} of hamster cheek pouch remained relatively constant as suffusion solution P_{O_2} was elevated from 10 to 47 mmHg, due to compensatory constriction of the arterial vessels. However, when the suffusate P_{O_2} was increased to 80 mmHg, oxygen levels increased significantly in the smaller arterioles and in tissue. Similarly, Prewitt and Johnson (96) found in certain preparations of the rat cremaster muscle using the microelectrode technique that the tissue P_{O_2} did not change when suffusate was changed from one equilibrated with 0% O_2 to 5 and 10% O_2 due to a decrease in red cell velocity and capillary density but did increase to 40 mmHg when suffusate oxygen level was increased to 21%. However, other preparations in the same study showed no change in red cell velocity or capillary density as suffusate O_2 concentration was altered. These "nonregulating" preparations had a very high tissue P_{O_2} of 59 mmHg compared with 19 mmHg in "regulating" preparations and appeared to be maximally dilated.

A discussion of the mechanisms responsible for this tendency for microcirculatory oxygen levels to remain constant with alteration in suffusate P_{O_2} is outside of the scope of this review, but it should be noted that it has been attributed to a number of factors. Early investigators suggested that vascular tone was regulated by the shift from aerobic to anaerobic metabolism (7), but tissue oxygen levels are generally considerably higher than the critical P_{O_2} of parenchymal cells obtained either in vitro or in vivo (99). It appears that several mechanisms at the level of the arteriole including nitric oxide, prostaglandins, and metabolites of cytochrome *P*-450 are involved in this response in different vascular beds (42, 80, 93). If these local regulatory mechanisms in the microcirculation are blunted by anesthesia, trauma of surgical preparation, or other factors, it is evident that the oxygen levels in the microcirculatory vessels as well as in the tissue would be altered.

The presence of local vasoregulatory mechanisms sensitive to oxygen levels described above is not sufficient to override the effect of other mechanisms that regulate blood flow. For example, increasing vascular tone by sympathetic nerve stimulation lowers blood flow and secondarily decreases P_{O_2} in the arterioles and tissue (9). The resultant fall in tissue P_{O_2} however does appear to cause a secondary relaxation of the arterioles and a partial return of oxygen levels.

While local control mechanisms appear to have the ability to compensate to a degree for effects of suffusate oxygen on oxygen levels in the microcirculation and the tissue, it would in general seem desirable to avoid any possible effects of this external factor. This is, however, unavoidable in invasive measurements of oxygen tension such as the oxygen microelectrode while this is not the case with optical methods such as the phosphorescence technique and the oxyhemoglobin saturation method.

XI. SIGNIFICANCE OF OXYGEN GRADIENTS

The gradients described above have in some cases been accompanied by hemodynamic data that made it possible to examine in greater detail the processes involved in oxygen loss from the microvascular network. These analyses, primarily of oxygen loss from the arteriolar network, have provided results that are not readily explained in terms of conventional concepts of oxygen delivery to the tissue.

A. Mass Balance Analysis of Oxygen Loss From the Microvessels

Swain and Pittman (123) carried out the first systematic experimental and analytical study of the decline of blood oxygen saturation in the arteriolar network of the hamster retractor muscle. They found that oxygen saturation of arterial blood decreases substantially for all orders of arteriolar branching and noted that " . . . flux of oxygen from the arterioles is much greater than would be expected by passive diffusion . . . " Based on the calculations of Kuo and Pittman (70), Swain and Pittman (123) indicated that the percentage of the measured longitudinal oxygen gradient that can be attributed to periarteriolar oxygen consumption ranges from 10% for A1 vessels to 35% for A4 vessels. Therefore, a balance ranging from 90 to 65% of oxygen was unaccounted for. Kuo and Pittman (70) calculated the maximum size of the Krogh tissue cylinder supplied by the arterioles and from this value determined the maximum longitudinal gradient. Comparing the calculated value with the measured values consistently showed that the calculated values ranged from 11 to 23% of the measured values, further supporting the concept of the existence of large oxygen sink that was not addressed by the methodology.

Specifically, Kuo and Pittman (70) found values of $4.9–8.4 \times 10^{-5}$ ml $O_2 \cdot s^{-1} \cdot cm^{-2}$ in 62- to 24-μm arterioles of the hamster retractor muscle using the three-wavelength spectrophotometric method. On the basis of these data, Popel et al. (94) indicated that the oxygen gradient that was needed to cause oxygen to leave the arterioles at the measured rates was of the order of 15 mmHg/μm, which is at least an order of magnitude greater than the tissue gradient that was presumed to exist in the tissue surrounding the microvessels, as inferred on the basis of the diffusion constant and solubility for oxygen in the tissue and the rate of oxygen consumption known to be prevalent in connective tissue and skeletal muscle.

Others also found unexpectedly high rates of oxygen loss from arterioles. Tateishi et al. (124) measured the rate of oxygen release from rat mesentery arterioles spectrophotometrically with a photon counting technique and averaging the results obtained at six different wavelengths. They carried out the experiments at 30°C and obtained an exit rate of 1.3×10^{-5} ml $O_2 \cdot s^{-1} \cdot cm^{-2}$. In the hamster skinfold, the rate of oxygen loss ranged from 4.1×10^{-5} ml $O_2 \cdot s^{-1} \cdot cm^{-2}$ in 64-μm first-order arterioles to 1.5×10^{-6} ml $O_2 \cdot s^{-1} \cdot cm^{-2}$ in 8-μm fourth-order arterioles (130). Popel et al. (95) found the value of 6×10^{-5} ml $O_2 \cdot s^{-1} \cdot cm^{-2}$, and Tsai et al. (132) obtained a value of 2.4×10^{-5} ml $O_2 \cdot s^{-1} \cdot cm^{-2}$ in 23-μm arterioles of the rat mesentery at 37°C using phosphorescence decay measurements. When these values are applied to the mass balance calculation, they invariably show the large imbalance between longitudinal and radial oxygen fluxes, a result that was also found theoretically by Secomb and Hsu (108). The excess oxygen exit from the arterioles when compared with the rate of diffusion that was calculated from the information available on the oxygen gradients in the tissue indicates that there is a systematic error in the calculation of the decrease of oxygen content in the arterioles, or that the gradients of P_{O_2} in the tissue could not be properly measured. Since all studies, using different measuring techniques, yield similar results on the decrease of oxygen content in the arterioles, the principal problem in the lack of mass balance is the measurement of oxygen gradients across the arteriolar wall.

The study by Tsai et al. (132) in the mesentery of the rat was critical in understanding the mechanism of this high rate of oxygen loss. This study utilized the phosphorescence optical technology to make an accurate mass balance between the decrease of oxygen content in the arterioles and the diffusional flux of oxygen out of the microvessels determined by the oxygen gradients in the surrounding tissue. These measurements provided for the first time a near simultaneous quantitative evaluation of the oxygen exit from microvascular segment and the tissue oxygen gradients that are the underlying reason for this flux. This study was also fundamentally different from previous studies on oxygen distribution because the animal was not anesthetized and the tissue was isolated from the environment, that is, not exposed to a suffusion solution that might influence the local oxygen levels.

The study of Tsai et al. (132) allowed to verify the accuracy of the data and calculations by application of the law of mass conservation (also called law of mass balance) that stipulates that the amount of O_2 lost from a vascular segment must be equal to the diffusional O_2 flux, determined by the perivascular P_{O_2} gradient. These investigators measured the rate of O_2 exit both longitudinally and radially in arteriolar vessel segments of the rat mesentery. Longitudinal saturation drop calculated from the P_{O_2} gradient was 2.4 ± 0.3%/100 μm in vessels with average diameter of 23 ± 3 μm and blood flow velocity of 1.5 ± 0.3 mm/s. Intravascular P_{O_2} was 43 ± 4 mmHg, and the difference between intravascular P_{O_2} and perivascular P_{O_2} was 18 ± 2 mmHg. Oxygen profiles in the tissue were obtained in the tissue surrounding the arterioles, as shown in Figure 5. The finding of a steep fall in P_{O_2} near the vessel wall was common to all groups. The measured tissue P_{O_2} profile in the region of the vessel wall was used to calculate the rate of oxygen exit by diffusion from the vessels, and this number was compared with the longitudinal rate of decrement of oxygen content of the same vessels. The average loss of oxygen from the moving blood was $2.4 \pm 0.5 \times 10^{-5}$ ml $O_2 \cdot s^{-1} \cdot cm^{-2}$, and the diffusion flow out of the same blood vessels calculated using the measured P_{O_2} gradient of 7 mmHg/μm was $2.2 \pm$

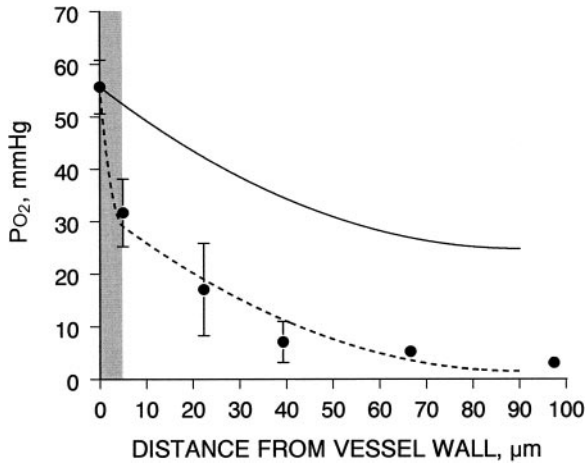

FIG. 5. P_{O_2} profile in the immediate vicinity of the arterioles in the rat mesentery. Fitting of these data to the oxygen profile deduced by solving the diffusion equation shows that the medium beyond the blood/tissue interface must be divided into two zones with significantly different rates of oxygen consumption, where the outside of the vessel wall rate is two orders of magnitude higher than the remainder of the tissue. The shaded area represents the portion of the tissue that is occupied by the vessels wall. [Data from Tsai et al. (132).]

0.2×10^{-5} ml $O_2 \cdot s^{-1} \cdot cm^{-2}$ in all of the vessels studied; thus the two calculations of oxygen loss agreed within 9%.

Hellums et al. (44) reviewed the methods of mathematical simulation of oxygen release from arteriolar size vessels. The work of this group has emphasized the importance of the resistance to oxygen transport in blood, pointing out that both the theoretical results by Nair et al. (83) and the experimental results in an in vitro system by Boland et al. (12) provide data in excellent agreement and that is significantly different from the predictions derived from Krogh tissue cylinder calculations. These investigators find that a red cell suspension flowing through a 27-μm-diameter cylindrical hole in silicon sheds oxygen at the rate of 3.5×10^{-5} ml $O_2 \cdot s^{-1} \cdot cm^{-2}$. Although this value is similar to the in vivo measurements, it cannot be compared because the permeability of silicon rubber is about seven times that of tissue (water) (35). Due to the high oxygen permeability, "the hole in silicon" model causes a rate of oxygen exit that is about one order of magnitude greater than that would be present if the hole were made in tissue-like gel, which is the argument that was used by Popel et al. (95) to attempt to explain the in vivo findings. The study of Buerk et al. (16) reported an oxygen loss of 2.4×10^{-6} ml $O_2 \cdot s^{-1} \cdot cm^{-2}$ in retinal arterioles, a rate of oxygen exit an order of magnitude lower than the previously discussed values since the gradient occurs in the vitreous, which is not consuming oxygen. These examples show that in one case the gradient is direct consequence of the high oxygen permeability properties of silicon, while in the second case it is a consequence of the lack of oxygen consumption in the surrounding tissue. Therefore, to explain the high rate of oxygen exit from arterioles, that do not have the high permeability to oxygen found in silicon, it is necessary to identify either an additional compartment that consumes oxygen or a mechanism that significantly increases the oxygen gradient at the blood/tissue interface.

It should be noted that the vessel wall oxygen consumption is a likely determinant in setting the wall oxygen gradient, since it is the only mechanism that increases the gradient by extracting oxygen from the tissue, thus lowering the tissue oxygen concentration in the region of the gradient. It should also be noted that large oxygen gradients are also possible if the blood/tissue interface constitutes a significant hindrance to the passage of oxygen. The later concept is the basis of the analysis of oxygen exit from the smallest arterioles and capillaries by Hellums et al. (44), who assume that in these vessels there is a red cell free boundary layer at the blood/tissue interface that presents a comparatively large resistance to oxygen transfer (33, 43). However, in this case, the cause for the resulting steep gradient, namely, high resistance to oxygen diffusion, would lead to a significantly lower rate of O_2 exit, as discussed in section XI*C*. This analysis also assumes that flow in the plasma layer is laminar and that there is no mixing, which is not likely since there is random motion of adjoining red blood cells.

B. Oxygen Distribution in the Vessel Wall

In attempting to explain the repeatedly observed large rate of oxygen exit from the arterial microcirculation, it is necessary to deal with the underlying physics of the problem, which is circumscribed by the following three parameters: *1*) the diffusion constant of oxygen in tissue, *2*) the local oxygen consumption of the tissue, and *3*) the solubility of oxygen in the tissue. These parameters in conjunction with a the specification of the geometrical features of the tissue and the appropriate boundary conditions in terms of P_{O_2} distribution describe the physical characteristics of this system and can be used to obtain a mathematical model of the processes involved.

Values obtained for the solubility of oxygen in the tissue are similar to that for water (81). In the absence of an active or facilitated transport mechanism, the diffusion constant of oxygen in tissue is determined by the diffusion constant of oxygen in water, which is very similar to water, since soft tissue is ~90% water.

Popel et al. (95) noted that the discrepancy between the measured oxygen loss from arterioles and the calculated diffusion flux in the tissue required that the vessel wall gradients be of the order of 15 mmHg/μm and indicated that " . . . the predicted and measured values can be made consistent with each other if we assume that permeability of the arterial wall is an order of magnitude higher . . . (than the range of values reported for most

tissues, i.e., $4.2–6.8 \times 10^{-10}$ ml $O_2 \cdot cm^{-1} \cdot s^{-1} \cdot mmHg^{-1}$). Permeability is defined as the product of the diffusion constant times the oxygen solubility; thus both factors could be in error when considering in vivo conditions. Pittman (89) addressed this issue suggesting that the permeability may be in fact higher by a factor of 2. 4 than the value conventionally used. Dutta and Popel (27) proposed that muscle tissue with high mitochondrial content may have higher than normal oxygen permeability. We should note that this does not explain findings in the mesentery by Tsai et al. (132) and in subcutaneous connective tissue by Kerger et al. (62). Furthermore, the concept of a higher vessel wall vascular permeability is not supported by the finding of Buerk et al. (15), who determined that the diffusion coefficient of the inner wall of arteries is ~50% lower than that of their outer wall.

Given these premises, the process by which oxygen is supplied to different tissues and organs is fundamentally determined by gradients of oxygen concentration. While this is evident for diffusion that drives oxygen out of the blood vessels, this same process also determines the existence of an equally important longitudinal oxygen concentration gradient in the circulation which is intertwined with the process of regulation of oxygen supply. Thus both longitudinal and transversal oxygen gradients are likely to be crucial determinants in tissue homeostasis and survival. It may be suggested that a possible role of the radial gradient could be that of protecting the tissue from the high P_{O_2} inherent of arterial blood, while the implicit high oxygen consumption which causes these large radial gradients may be a reflection of the convenience or necessity of locating a tissue of very high energy consumption in the immediate proximity of the energy source, i.e., arterial blood as shown in Figure 6. The longitudinal gradient may also have a specific role in the regulation of blood flow and tissue oxygenation as shown by the relationship between the adrenergic innervation in the arterioles, which is maximal in the A2 and A3 arterioles, and the distribution of oxygen in the microcirculation and the position of the inflection in the dissociation curve for hemoglobin which suggest that the A2 and A3 arterioles may play a crucial role in regulation and that the microcirculation may be adapted to a particular distribution of partial pressure of blood as shown in Figure 7.

C. Dependence of Results on Measurement Techniques Used

Several attempts have been made to attribute the measurement of large rates of oxygen exit in vivo to methodological errors. Pittman (89) proposed that the flow and oxygen profiles in the arteriolar lumen may give an overestimate of the oxygen exit from the moving blood. However, this large rate of oxygen exit has been measured utilizing a variety of techniques.

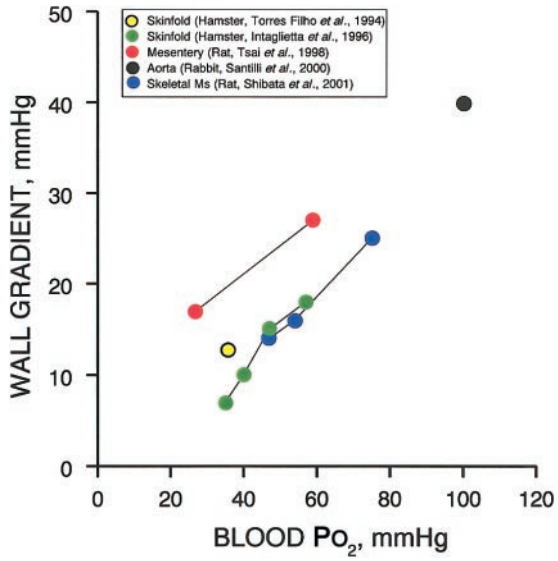

FIG. 6. Difference in oxygen tension across the arteriolar wall/endothelium as a function of blood P_{O_2}. The trend of the data suggests that the difference in P_{O_2} that is directly proportional to the rate of oxygen consumption near the endothelial layer of the vessel wall is a function of the blood P_{O_2} that is in contact with the endothelial layer.

Recently, it has been proposed (135) that there is most likely a systematic error in the calculation of oxygen loss, since the vascular wall O_2 consumption required to produce the observed results is about two orders of magnitude higher than seen in most in vitro studies of oxygen consumption of arterial segments or endothelial cell cultures. That study proposes that a systematic error at the upstream site, either in flow measurement or oxygen saturation or both, due to the proximity of this site to a branch point, is most likely introducing an error into the estimate. However, the upstream site in such studies is not always immediately downstream from a branch point. For example, the studies of Tsai et al. (132) utilized arterioles of rat mesentery that are long and straight, with infrequent branches. In addition, the flow measurements in these studies are not always taken at the upstream site. In the studies of Seiyama et al. (109), the flow measurements were obtained over the entire length of the vessel segment in which oxygen saturation was measured. It is also suggested by Vadapalli et al. (135) that the estimate is based on small differences in large values and therefore may be in error. However, in some studies, the drop in oxygen saturation or P_{O_2} is substantial, and changes of 10% or more are not unusual.

Vadapalli et al. (135) also suggest that all measurements of oxygen exit based on mass balance calculations are biased because of a systematic error produced by a mechanism that overestimates the upstream oxygen influx relative to the downstream efflux, because the bifurcations that supply oxygen to the vessels produce effects that are greater in the upstream location, while the bifur-

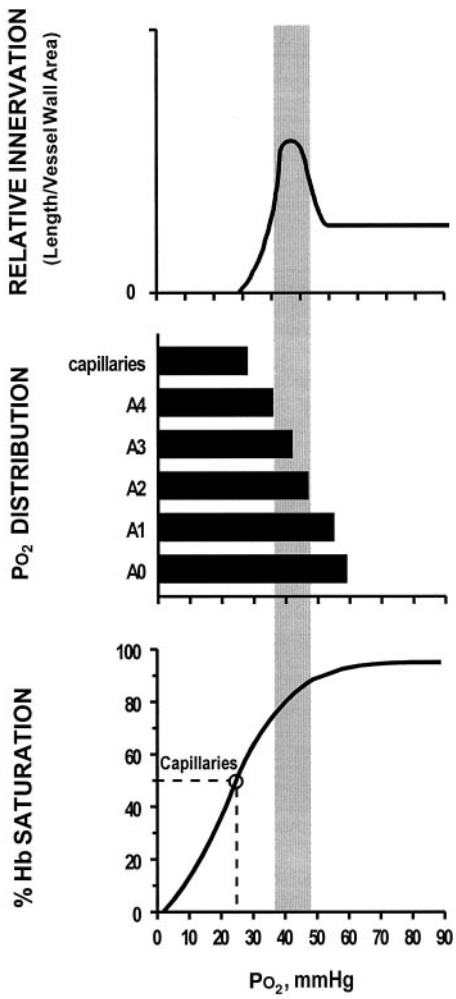

FIG. 7. Microvascular distribution of oxygen partial pressure as a function of adrenergic innervation of the arteriolar wall (102) and the shape of the oxyhemoglobin dissociation curve. The placement of the "knee" of the oxygen dissociation curve in the vessels with the highest density of adrenergic enervation suggests that the arteriolar microvasculature is adapted to a specific distribution of oxygen partial pressures which serves as a signal for controlling microvascular function. [P_{O_2} distribution from Intaglietta et al. (51); %Hb saturation from Ulrich et al. (134).]

cation that leaves the vessel probably has no effect on the oxygen distribution in the vessel segment being studied. This argument is unlikely to be correct if we consider the physics of the problem and the measuring techniques utilized. If there were a nonuniform velocity profile due to the exit of peripheral low-velocity fluid at a bifurcation, due to laminar flow, the bifurcation would cause an asymmetric flow velocity increase on the side of flow exit. Because velocity measurements are invariably made in the vessel centerline, the presence of an asymmetric peripheral high-velocity flow would not be detected, causing a systematic underestimate of the upstream convective oxygen entrance into the vessels, which is the opposite of the hypothesis of Vadapalli et al. (135). A similar argument indicates that if there is an oxygen saturation profile in a blood vessel, where physical conditions dictate that oxygen saturation is lower at the periphery than the core, then a bifurcation would extract low saturation blood from the periphery, shifting the location of maximum saturation away from the centerline. Also as a consequence of the Fåhraeus effect the red blood cell concentration changes at bifurcations, possibly producing a high hematocrit in the streamlines adjacent to the bifurcation, which would again underestimate the amount of oxygen entering the test segment if this is evaluated at the centerline. Thus most phenomena associated with effects downstream of bifurcations tend to underestimate the amount of oxygen entering the vessel segment since measurements are always made in the centerline. Again, since measurements are usually made in the centerline, the net effect is that the oxygen influx is underestimated. Both the asymmetry in velocity and in oxygen saturation profiles are additive and produce an underestimation of the upstream oxygen influx. Conversely, there is no mechanism for increasing centerline velocity or oxygen saturation in the straight vessels usually chosen for this type of analysis that can lead to an overestimation of the upstream oxygen influx.

The parameter sensitivity analysis reported by Vadapalli et al. (135) is only meaningful if measurement errors are assumed to be random. Because these measurement errors are equally likely to occur upstream and downstream, this work highlights the fact that conclusions in this type of mass balance analysis can only be drawn when two independent methods of measurement reach the same result, as for instance in the study of Tsai et al. (132), described above, where the rate of oxygen exit calculated by mass balance was found to match the rate of oxygen exit determined by diffusion measurements. Application of standard statistical methods to this result shows that the hypotheses tested, namely, that the rate of oxygen exit measured by mass balance is the same as the rate of diffusion (due to the large vessel wall gradients), has a probability >95% of being correct.

It has been suggested that the presence of a steep P_{O_2} gradient near the blood/vessel wall interface in arteries may be due to the slow diffusion through an unstirred layer in the blood immediately adjacent the vessel wall (91, 101). However, the existence of a significant unstirred layer of blood or plasma in a dog carotid artery of ~2 mm I.D. with a mean flow of 100 ml/min (53) would seem to be problematic since the wall shear rate would be $\sim 2.1 \times 10^3$ s^{-1}. Moreover, an unstirred layer would not present the steep gradient seen in these studies. A second possible explanation for the steep gradient is the localized depletion of oxygen from the peripheral blood layer due to its lower hematocrit [the wall exclusion effect, Maude and Whitmore (79)]. In this case, a standing difference in P_{O_2} of 40 mmHg over a distance of 5 μm or less would be present in the flowing blood near the wall. Finally, both of

these explanations preclude the existence of a high rate of oxygen exit since they postulate increased resistance to diffusion.

Recent data by Goldsmith et al. (38), however, suggest that collisions and deformation of red blood cells in shear flow lead to random radial displacements which introduce a process of solute mixing even though the flow is laminar. Under these conditions the oxygen concentration profile in microvessels should be fairly uniform up to the blood/tissue interface, which should effectively eliminate any resistance to oxygen transfer. This conclusion is based on substantial prior experimental evidence and analytical studies showing that the molecular diffusivity of materials dissolved in plasma is significantly augmented by red cell rotation and motion in the shear field characteristic of blood flow in the microcirculation. The work of Keller and Friedlander (59), Diller and Mikic (23), and Zydney and Colton (148) indicate that this augmentation doubles the diffusional transport. Consequently, the presence of a high resistance to oxygen transport on the luminal side of the arterioles is not likely, and since physical principles do not support the hypothesis of very high diffusivity in the vessel wall suggested by Popel et al. (94), we are left with the possibility of the existence of larger than normal perivascular gradients that cause the high rate of oxygen extraction.

D. Rate of Oxygen Loss

In some of the studies cited above, data obtained on hemodynamic parameters as well as changes in P_{O_2} or HbO_2 saturation over a known distance made it possible to calculate the rate of oxygen loss from the blood as it coursed through the arterioles. Initial calculations by Ellsworth et al. (28), in hamster cheek pouch arterioles, using periarteriolar P_{O_2} as representative of intravascular values, revealed that the rate of oxygen loss was about two orders of magnitude higher than would be expected from diffusion. These results caused Popel et al. (94) to suggest as a possible explanation that the diffusion coefficient might be much higher than the norm for tissue in the arteriolar wall, although the other possible explanation, namely, that the O_2 consumption of the vessel wall might be higher than expected, was also noted. In subsequent tests of the high diffusion coefficient hypothesis, evidence was obtained that the coefficient might be two times that found in aqueous media, possibly reflecting the increased solubility of oxygen in the lipid bilayer of the cell membrane (6), but still much lower than required to explain the rate of oxygen loss by the arteriole. In retrospect, it is apparent that this untenable hypothesis was formulated because the data on the actual P_{O_2} gradients in the tissue were obtained with microelectrodes which, as a consequence of the catchment volume, may significantly underestimate the wall gradient because they average into the measurement the high values of the blood P_{O_2}.

Calculations of the rate of oxygen loss from arterioles based on measurements of HbO_2 saturation produced similarly high rates of loss (70). Subsequent studies using the phosphorescence technique, as described above, to measure the intravascular P_{O_2} in the skinfold preparation of the awake hamster showed a similar rate of oxygen loss (51, 132), and those investigators proposed that a high O_2 consumption of the wall was responsible.

E. Calculation of the Rate of Oxygen Consumption of the Arteriolar Vessel Wall

The large rate of oxygen exit from arterioles requires a commensurate diffusional flux out of these vessels and therefore an appropriate gradient to drive this flux. Based on the considerations given above, the steep gradients of oxygen concentration across the wall can only be the result of a significant oxygen consumption within the confine of the vessel wall, since these steep gradients are not evident elsewhere. The magnitude of oxygen consumption required for these gradients was estimated by Duling et al. (26) to be 1.7 ml $O_2 \cdot min^{-1} \cdot g\ tissue^{-1}$ from measurements using microelectrodes, which is one hundred times the oxygen consumption of connective tissue or skeletal muscle at rest. Duling and co-workers (26) commented that "... the value of consumption by the wall elements is far in excess of the values actually measured for vascular smooth muscle." They did not dismiss their finding of a large wall gradient as an experimental artifact and noted that "... the enzymes related to oxidative phosphorylation increase along the vascular tree and such a variation could affect the transmural gradients." Since the wide range of biochemical activities of the endothelium was not known at that time, this possibility was not explored further.

Tsai et al. (132) calculated the oxygen consumption needed to obtain the oxygen gradient found in the vessel wall of 30- to 50-μm-diameter arterioles in the rat mesentery and obtained the value of 3.9 ml $O_2 \cdot min^{-1} \cdot g$ arteriolar wall $tissue^{-1}$. With the use of the same technique, the rate of oxygen consumption of a region of mesenteric tissue adjacent to the microvessels but devoid of microvessels was found to be 1.4×10^{-2} ml $O_2 \cdot min^{-1} \cdot g^{-1}$, a value which is not greatly different from data obtained for loose connective tissue in other animals when scaled according to size. These results lead to the conclusion that the large longitudinal oxygen loss from the arterioles is in part due to their very high rate of oxygen consumption.

Given the finding of the existence of this significant oxygen sink, it is of interest and important to determine what is its relative magnitude vis á vis the total oxygen

consumption of the organism. Order of magnitude estimates can be obtained with two different approaches. First, the present results indicate that the rate of oxygen consumption of these vessels is ~100–200 times that of all other tissues. The additional element of information required is the amount of tissue represented by the arterioles of the organism, a parameter not known with certainty. Using the data of Mall [cited by A. C. Burton (18) and Paul (88)], it can be estimated that small arteries and arterioles between 600 and 10 μm diameter comprise 5% of the vascular volume, and since in general the vessel wall thickness to diameter ratio for the vasculature is ~20%, the actual volume of the vascular walls is 40% of the vascular volume; thus the mass of arterioles in the circulation is ~2% of the vascular volume. Because vascular volume for most species is ~8% of the body mass, the mass of arterioles in the body represent ~0.16% of the whole body mass (18). In this scenario, if arterioles consume ~150 times more oxygen than other tissues, they are responsible for using ~24% of the total oxygen consumption of the body (at rest).

Although speculative, these calculations are indicative of a very large rate of consumption of oxygen of the arterioles, and if this were adversely modified, i.e., the total oxygen supplied were to diminish while arteriolar consumption were to remain constant, this could lead to reduced, or in extreme circumstances precarious oxygenation conditions for the organism as a whole, but not necessarily for the arterioles since they are at the beginning of the oxygen supply line.

XII. ESTIMATES OF OXYGEN CONSUMPTION OF THE VASCULATURE

An extensive review of the respiration of vascular tissue was carried out by Paul (87). The data were mostly derived from isolated vessel segments, slices, or rings and focused in the respiration rate of smooth muscle, with no particular attention to the status of the endothelium. The consensus of this work is that although there is a significant variability in results, the majority of measured values lie between 1.1 and 4.5×10^{-3} ml $O_2 \cdot min^{-1} \cdot g^{-1}$; as discussed in what follows, these numbers are as much as three orders of magnitudes smaller than measurements related to the respiration of arterioles in whole organs, with intact endothelium.

A. Organ Studies

Two systemic and whole organ studies provide some indication of the oxygen respiration of the vasculature in vivo. Curtis et al. (22) used a detergent to strip the endothelium of the blood vessels of the dog hindlimb and found that oxygen consumption of the preparation decreased by 35%. These authors explored a number of alternatives to explain the decreased oxygen consumption. The removal of endothelium can in principle cause tissue edema, since the endothelium is the semipermeable membrane that determines the interplay between oncotic and hydraulic forces that balance fluid exchange according to the Starling hypothesis (52), and edema may interfere with oxygen extraction by increasing the oxygen diffusion path length. However, dry to wet samples of muscle showed that there was no edema present. A different concern was whether endothelial debris produced by the detergent plugged capillaries, lowering functional capillary density. This was scrutinized by microscopic histological studies which showed no evidence for plugged capillaries. Given the results of this study, if we assume that the endothelium is on the order of 0.1% of the tissue mass, we may conclude that the oxygen consumption of this tissue in situ is ~350 times that of the remainder of the tissue, an estimate of the same order magnitude of that of Tsai et al. (132).

The study of Ye et al. (146) provides a special insight on the potential consumption of the microvasculature and particularly the arterioles. These authors perfused the rat hindlimb, kidney, intestine, and mesentery at constant flow and found that vasoconstriction induced by the administration of norepinephrine or vasopressin significantly increases oxygen consumption, i.e., the amount of oxygen extracted from the perfusion solution. This study indicated that perfused blood vessels in the mesentery consumed oxygen at the rate of 115 mol $\cdot h^{-1} \cdot$ g wet wt^{-1} of blood vessels at 25°C and that this value increased by 75% upon constriction. In comparison, these authors report that the basal oxygen consumption of the rat hindlimb is 14.5 ± 0.3 mol $\cdot h^{-1} \cdot$ g hindlimb^{-1}. It should be noted that vasoconstriction per se lowers tissue perfusion in terms of functional capillary density (131); therefore, it is not likely that the increased oxygen consumption was due to a better perfusion of the tissue, although the authors favored that interpretation in later studies (126, 127). Furthermore, the mediators act on the resistance arteries and arterioles, which represent ~11% of all blood vessels, where it is estimated that the weight of small arteries and arteriolar vessels involved in controlling blood flow is of the order of 0.4% of the whole body mass. [Note: Paul (87) indicates that the total vascular mass of the organism is 3.4%; thus arterioles are estimated to be ~10–15% of this mass.]

These investigators (146) noted that vasoconstriction of the hindlimb, as evidenced by blood pressure increasing by ~120 mmHg from basal values (90 mmHg) at constant perfusion, caused oxygen consumption to increase by 9 mol $\cdot h^{-1} \cdot$ g hindlimb^{-1} (3.4×10^{-3} ml $O_2 \cdot$ min$^{-1} \cdot$ g hindlimb^{-1}). If we assume that this work represents the energy expenditure of the arterioles and small arteries or ~0.4% of the tissue, then the additional work of

contraction causes these vessels to consume oxygen at the rate of 0.9 ml $O_2 \cdot min^{-1} \cdot g$ vessel $wall^{-1}$. This value is about one-half of that found by Tsai et al. (132), and because this would appear to be the oxygen required by the arteriolar vasculature to achieve normal tone, we may conclude that these levels of oxygen consumption are indicative of the general expenditure of oxygen required by the arterioles in maintaining normal tone. Evidence for a significant oxygen consumption by the arterioles was also found by Marshall and Davies (78), who studied oxygen consumption of the hindlimb of the rat adapted to chronic systemic hypoxia and found that when these rats breathed room air the oxygen consumption was 0.006 ml $O_2 \cdot min^{-1} \cdot g$ $hindlimb^{-1}$ greater than that of normal (nonadapted) rats. This significant change was attributed to the increase in consumption by the vascular tissue, corresponding to an increase of 0.18 ml $O_2 \cdot min^{-1} \cdot g^{-1}$. These investigators used the figure of 3.4% as the proportion of vascular tissue to whole tissue mass indicated by Paul (87); however, if we assume that this oxygen consumption occurs mainly in the arterioles which represent only of the order of 0.4% of the tissue mass, then the oxygen consumption of the arterioles would increase by 1.53 ml $O_2 \cdot min^{-1} \cdot g^{-1}$, which is similar to that of Tsai et al. (132).

The work of Curtis et al. (22) and Ye et al. (146) supports the concept of a high oxygen consumption by the endothelium and the arterial and arteriolar vasculature as it develops tone; however, the results are not internally consistent regarding the effects of vasoconstrictors. In the study of Curtis et al. (22), vasoconstriction in the perfused hindlimb of the dog was induced at constant flow by the administration of N^G-nitro-L-arginine methyl ester (L-NAME; 20 mg/kg body wt) plus indomethacin (3mg/kg bw), and this caused the decrease of oxygen extraction. Conversely, in the study of Ye et al. (146), the administration of 0.1 nM vasopressin by constant infusion at a rate of 1% of the rate of perfusion caused the increase of oxygen uptake, an effect that was also found with the infusion (at the same rate) of 3 nM epinephrine. This disparity in the effects of vasoconstrictors on oxygen uptake may be due to the different mediators used. However, the fact that Curtis et al. (22) did not find an increase in oxygen uptake when using L-NAME is particularly puzzling in view of studies by Shen and co-workers (110, 111), which indicate that basal levels of nitric oxide are needed to lower oxygen consumption by the tissues, which increases when nitric oxide is either scavenged or nitric oxide production is interfered with. These discrepancies may be due to methodological differences, since Ye et al. (146) perfused their preparations with a Krebs-Ringer bicarbonate solution containing 2% bovine serum albumin warmed to 25°C, which is an acellular solution of very low viscosity, while Curtis et al. (22) perfused their preparation with whole blood. Perfusion of a vasoconstricted tissue with blood causes a significant decrease in functional capillary density (61), namely, number of capillaries through which there is passage of red blood cells, downstream from the vasoconstricted vessels (133). Given the difference in oxygen-carrying capacity of a factor of ~20 between blood and a plasma, it is probable that the experiment of Curtis et al. (22) reflects the change in capillary perfusion by red blood cells (which carry most of the oxygen), while in the experiments of Ye et al. (146) there is no decrease in perfused capillary density since their low viscosity perfusate permeates the whole microcirculation unless capillaries become 100% occluded, which is unlikely. This analysis is relevant because it is likely that in the case of Curtis et al. (22), the principal oxygen carrier (red blood cells) is partially excluded from the capillaries once the vasoconstrictor is introduced, whereas in the case of Ye et al. (146), the same oxygen carrier continues to perfuse the capillaries unless they become totally obstructed.

B. In Vitro Measurements of Oxidative Metabolism

In vitro techniques have been used by a number of investigators to determine the oxygen consumption of segments of arteries and arterioles as well as of isolated endothelial and smooth muscle cells. The first report on the respiration of isolated arterioles appears to be the study of Howard et al. (49), who utilized the Cartesian diver technique and found that cheek pouch or mesentery arterioles (65–150 μm diameter) consumed oxygen at the rate of 0.1 ml $O_2 \cdot min^{-1} \cdot g^{-1}$. This value is similar to that found by Sussman et al. (122) in isolated cerebral microvessels where O_2 consumption ranged from 0.03 to 0.09 ml $O_2 \cdot min^{-1} \cdot g^{-1}$.

Data on oxygen consumption of the endothelium were first obtained by Bruttig and Joyner (13), who used a manometric method to determine respiration and found that a culture with a cell density of 6×10^5 cells/5 cm^2 consumed oxygen at the rate of 2.5×10^2 ml $O_2 \cdot min^{-1} \cdot g^{-1}$. These authors noted that the rate was significantly out of proportion with oxygen consumption of the organism and indicated that " . . . organized tissue can inhibit potential cellular metabolism as much as 5,000-fold." Subsequent studies by Kjellström et al. (64) found that oxygen consumption of the endothelium in cell cultures ranged between 1.6 and 8×10^{-2} ml $O_2 \cdot min^{-1} \cdot g^{-1}$ depending on origin and species, and Motterlini et al. (82) found the value of 5.6×10^{-2} ml $O_2 \cdot min^{-1} \cdot g^{-1}$ for endothelial cells from the pig aorta.

Helmlinger et al. (45) measured P_{O_2} profiles in a sandwich model for the study of cell cultures in vivo, in which endothelial cells are grown between two glass plates in such a fashion that they receive oxygen from the environment from the edges of the sandwich. The phos-

phorescence decay method was used to obtain oxygen concentration profiles in the chamber, starting from the periphery which is exposed to ambient air. The change in P_{O_2} as one progresses inward from the periphery is due to oxygen consumption and defines the penetration length or distance over which the cells have sufficient oxygen to remain viable. Applying the solution of the diffusion equation to the data reported for this system, and considering previous reports indicating that oxygen limitation progressively and spatially reduces cell viability in this model (46), we find that these cells consume oxygen at a rate of 0.22 ml $O_2 \cdot min^{-1} \cdot g^{-1}$. These data were collected at room temperature (20°C). Correcting this value to that at 37°C, according to the algorithm of Altman and Ditter (2), we obtain the value of 1.2 ml $O_2 \cdot min^{-1} \cdot g^{-1}$.

It is apparent that oxygen consumption from cell cultures is highly dependent on the method of measurement and is probably not representative of the conditions in vivo. Vadapalli et al. (135) made a comprehensive review of the results obtained in evaluating the oxygen consumption of endothelial cells in culture and noted that, with the exception of the study of Bruttig and Joyner (13) and Kuehl et al. (69), the studies in the literature report that oxygen consumption of this cellular species is about two orders of magnitude lower than that shown by the in vivo studies. Vadapalli et al. (135) also indicated that with the exception of the study Tsai et al. (132) there are no measurements in vivo of both the intraluminal and perivascular P_{O_2} needed to determine the oxygen consumption of the vessel wall. However, studies by Duling et al. (26) and Santilli et al. (105), who determined all the necessary parameters for measuring vessel wall oxygen consumption in vivo, obtained values that fully support the finding of Tsai et al. (132).

Calculation of oxygen consumption of the endothelial layer in the blood vessels can be made using the solution of the diffusion equation in Cartesian coordinates, which is a simplified approximation. According to Tsai et al. (132), the oxygen consumption g_o (in ml $O_2 \cdot min^{-1} \cdot g\ tissue^{-1}$) is given by

$$g_o = \left[\frac{\partial P_{O_2}}{\partial x}\right]_{x=0} \frac{D\alpha}{\delta}$$

where the bracketed expression is the gradient of oxygen tension at the blood vessel wall interface (in mmHg/cm), D is the diffusion constant for oxygen in the vessel wall (1.7×10^{-5} cm^2/s), α is the solubility of oxygen in the vessel wall (2.1×10^{-5} ml $O_2 \cdot mmHg^{-1} \cdot cm^3$ $tissue^{-1}$), and δ can be approximated to be the thickness of the vessel wall. With the use of this approximation, the consumption of oxygen of the vessel wall (endothelium) deduced from the work of Tsai et al. (132) is 4.5 ml $O_2 \cdot min^{-1} \cdot cm^3$ $tissue^{-1}$ (instead of 3.9 obtained with exact calculation). Using the data of Duling et al. (26), we obtain the value of 0.1 ml $O_2 \cdot min^{-1} \cdot cm^{-3}$ for arterioles of similar dimension (22 μm diameter). The results of Santilli et al. (105) for the rabbit aorta yield the value of 1.6 ml $O_2 \cdot min^{-1} \cdot g\ tissue^{-1}$ if we assume that the metal tip electrodes used have a catchment volume of 1–2 μm diameter and δ is on the order of 30 μm wall thickness oxygenated by oxygen diffusing from the bloodstream, as shown in their data. Buerk and Goldstick (14) carried out a similar study with electrodes ranging from 10 to 200 μm tip diameter. As we might expect due to the much larger tip diameter, they could not detect the very sharp gradient of oxygen tension across the endothelial layer. However, model calculations made on the basis of the measured profiles determined that the inner wall of arterial vessel consumed oxygen at a rate that was ~16 times that of the outer surface, obtaining the value of 0.078 ml $O_2 \cdot min^{-1} \cdot g\ tissue^{-1}$. They stated that " . . . the most likely explanation for the observed asymmetry in P_{O_2} profiles is a higher oxygen consumption near the endothelium" and attributed this effect to the synthesis of prostacyclin in the inner wall (34). In a subsequent study (15) they found that the diffusion coefficient near the outer wall was ~50% lower than that of the outer wall, which lowered the rate of consumption of the outer wall (tissue containing the endothelium) to be about eight times that of the outer wall (tissue not containing endothelium). In summary, these results show substantial variability, particularly due to the uncertainty in δ. Nonetheless, they are in the range of one to two orders of magnitudes higher than for most tissues. Given that findings with cell cultures, in general, report that the rate of oxygen consumption of endothelium is about two orders of magnitude lower than that shown by in vivo, in situ, studies, we conclude that in vivo conditions and processes appear to be fundamentally different from those in cell culture. In summary, these results show substantial variability, particularly due to the uncertainty in δ.

C. Possible Mechanisms of Elevated Oxygen Consumption in Arterioles

A large oxygen consumption should be evident in terms of measurable biological activity. In the case of endothelium, although the mitochondrial density of endothelial cells is not very high, many of the biochemical functions of these cells require oxygen (64). Furthermore, the measurements of oxygen consumption of endothelium by Bruttig and Joyner (13) show that these cells are capable of oxygen consumption rates that can be as much as three orders of magnitude higher than most cells. The biochemical functions of these cells include synthesis and secretion of renin, prostaglandins, collagen, endothelin, prostacyclin, endothelium-derived relaxing factor, inter-

leukin, factor VIII, degradation of bradykinin and prostaglandins, clearance of proteins, lipids and lipoproteins, conversion of angiotensin I to II, and expression of antigens. Smooth muscle may also participate in this metabolic process, although a steady level of contraction may be maintained at least in part by a non-energy-consuming latch mechanism. It should be noted that if such a ratchetlike mechanism were in operation only it saves energy in steady contraction, and not in conditions of steady-state variability of microvessel diameter, termed vasomotion, which is consistently observed in in vivo investigation of the microcirculation (8).

In vitro studies of vascular smooth muscle generally reveal oxygen consumption levels that are also in the range seen in most studies of endothelium, described above. For example, Motterlini et al. (82) reported a rate of oxygen consumption of 0.022 ml $O_2 \cdot min^{-1} \cdot g^{-1}$ for vascular smooth muscle cells in suspension or somewhat less than one-half that reported above in endothelial cells by these investigators. This observation is consistent with the values found in isolated arterioles of 0.030–0.100 ml $O_2 \cdot min^{-1} \cdot g^{-1}$ cited above (49, 122). In addition, it should be noted that the energy cost of smooth muscle contraction as measured in vivo is much less than that of skeletal muscle (88).

D. Contribution of Capillary and Venular Endothelium to Vascular Oxygen Consumption

Considering that the large rate of oxygen consumption of the arteriolar vessel wall is most likely due to the activity of the endothelium, we must consider that endothelial cells are present in much greater numbers, due to the greater surface area, in the capillary system and the venular system. The fact that gradients can be detected in the capillaries of the hamster skinfold tissue is significant. Also, it is notable that as we progress from the smaller to the largest venules, the wall gradient for oxygen increases. In the absence of mass balance data, it is not possible to determine whether this gradient reflects a substantial degree of oxygen consumption or a barrier to oxygen release, although based on findings in the arterioles the former must be considered more likely. Based on this premise, the oxygen radial gradient of capillaries as shown in Figure 4 may be considered representative of the basal oxygen requirement of the capillary microvascular endothelium. These observations raise certain questions regarding the resting levels of capillary and venular P_{O_2} and the factors that determine them. Although it may be speculative, the consistent observation of a higher mean oxygen level in the distal venules raises the possibility that this feature may serve a functional purpose related to the oxygen requirements of these vessels. This may be more evident in tissues with low oxygen requirements such as the hamster skinfold where the primary function of the capillaries may be that of providing an adequate surface area per unit volume of tissue for facilitating the extraction of the products of metabolism. Thus it will be important in future studies to examine more closely the oxygen levels and gradients of the capillaries and venules to better understand their function. The possibility that oxygen reaches the venules in part by diffusion from the arterioles rather than by convection should be included in this consideration.

XIII. CONCLUSIONS

Although blood oxygenation takes place in lung capillaries, data on longitudinal and radial oxygen gradients in the arteriolar blood vessels of most tissues suggest that a significant amount of oxygen is lost from these vessels, with the result that in some tissues the oxygen supplied by capillaries is secondary to that provided by the arterioles. The fractional oxygen loss in the arteriolar network depends on the metabolic activity of the organ involved, with the gradient being steepest in organs with low rates of metabolic activity. Conversely, tissues with high metabolic activity and corresponding higher rates of blood flow exhibit relatively shallow oxygen gradients in the arteriolar network. In tissues with low rates of metabolic activity, the arteriolar network appears to be the main site of oxygen delivery to the tissues. In addition, in the latter case, the rate of oxygen loss from the arterioles is too large to be explained by diffusion alone, unless it is assumed that oxygen diffusivity is an order of magnitude higher than reported for other tissues. However, the P_{O_2} drop across the arteriolar wall is much greater than would be predicted from very high diffusivity. The only explanation, apart from an unlikely combination of measurement errors, is that the oxygen consumption of the arteriolar wall in vivo is about two orders of magnitude higher than would be expected from in vitro studies of endothelium and vascular smooth muscle. Since it is known that the endothelium is responsible for synthesizing a wide variety of autacoids important in vascular function, it is possible that the oxygen requirements of these pathways are much higher in vivo than in vitro. The functional significance of this extraordinarily high metabolic rate of the arteriolar vessel wall remains to be determined, but it may provide a metabolic barrier to protect the parenchymal tissue from the high oxygen level of arteriolar blood and, for example, greatly reduce the formation of oxygen free radicals in the perivascular tissue (5, 76). In this context, it should be noted that the radial oxygen gradient and therefore the rate of oxygen consumption of the blood/tissue interface for all vessels is directly proportional to

the level of blood oxygen as shown in Figure 6. Major issues to be addressed in the future are the physiological significance of this process, the biochemical mechanisms that cause the high rate of oxygen consumption in the arteriolar wall, and the potential for this mechanism to be a factor leading to ischemic conditions, for example, in low flow states.

In terms of a unifying general scheme, it may be that in organs where oxygen diffusion from the arterioles is a major source of tissue oxygen, there is apparently a balance between the consumption of the wall and the supply of oxygen to the surrounding tissue such that these tissues are not exposed to the oxygen levels found in the arteriolar lumen but the tissue P_{O_2} is sufficient to support oxidative metabolism.

Radial gradients are steepest in the tissues surrounding the arterioles, less so in the capillary region, and lowest in the vicinity of the venules. Longitudinal and radial gradients in the capillary network also show a dependence on the metabolic rate of the tissue, being more pronounced in brain and exercising muscle than in resting skeletal muscle and mesentery. In fact, at the highest rates of metabolic activity studied, virtually all the fall in blood oxygen levels appears to occur across the capillary bed. There is evidence of a significant oxygen gradient within the capillary itself, which may be a limiting factor in skeletal muscle at high metabolic rates.

Measurements of radial gradients in the vicinity of the venules indicate that there is additional loss of oxygen from the venular network. Despite this, the mean P_{O_2} of the distal venules is generally higher than the postcapillary vessels, principally in tissues with low metabolic activity, and is likely due both to a convective shunt in which high flow pathways in the capillary network and small venules also have higher P_{O_2} levels and a diffusional shunt from arterioles to venules. In tissues with higher metabolic rates, there is relatively little change in the P_{O_2} along the venular network. If there is functional significance to this phenomenon, it may be speculated to be in terms of assuring a certain level of oxygen in the larger venules and veins.

It is important to acknowledge that the current database on oxygen gradients in the microcirculation is far from complete and that only a small number of the studies cited were undertaken specifically to determine P_{O_2} gradients and to examine the mechanisms underlying the creation of these gradients. As a consequence, many significant issues regarding the underlying mechanisms that determine oxygen gradients in the tissues during normal activities remain to be explored. Considering the paramount importance of oxygen delivery to the tissues, exposing this lack of knowledge may stimulate new efforts to obtain a more complete understanding of this area and resolve current controversies.

This work was supported by National Heart, Lung, and Blood Institute Bioengineering Partnership Grant R24-HL-64395 and Grants R01-HL-62354, R01-HL-62318, and R01-HL-66318.

Address for reprint requests and other correspondence: M. Intaglietta, Dept. of Bioengineering, Univ. of California, San Diego, 9500 Gilman Dr., La Jolla, CA 92093–0412 (E-mail: mintagli@ucsd.edu).

REFERENCES

1. Algire GH. An adaptation of the transparent chamber technique to the mouse. *J Nat Cancer Inst* 4: 1–11, 1943.
2. Altman PL and Ditter DS. *Respiration and Circulation*. Bethesda, MD: FASEB, 1971.
3. Altman PL and Ditter DS. *Biology Data Book*. Bethesda, MD: FASEB, 1974.
4. Asher EF, Alsip NL, Zhang PY, and Harris PD. Prostaglandin-related microvascular dilation in pentobarbital- and etomidate-anesthetized rats. *Anesthesiology* 76: 271–278, 1992.
5. Bauer V and Bauer F. Reactive oxygen species as mediators of tissue protection and injury. *Gen Physiol Biophys* 18: 7–14, 1999.
6. Bently TB and Pittman RN. Influence of temperature on oxygen diffusion in hamster retractor muscle. *Am J Physiol Heart Circ Physiol* 272: H1106–H1112, 1997.
7. Berne RM. Regulation of coronary blood flow. *Physiol Rev* 44: 1–29, 1964.
8. Bertuglia S, Colantuoni A, Coppini G, and Intaglietta M. Hypoxia- or hyperoxia-induced changes in arteriolar vasomotion in skeletal muscle microcirculation. *Am J Physiol Heart Circ Physiol* 260: H362–H372, 1991.
9. Boegehold MA and Johnson PC. Periarteriolar and tissue P_{O_2} during sympathetic escape in skeletal muscle. *Am J Physiol Heart Circ Physiol* 254: H929–H936, 1988.
10. Bohlen HG. Tissue P_{O_2} in the intestinal muscle layer of rats during chronic diabetes. *Circ Res* 52: 677–682, 1983.
11. Bohlen HG and Lash JM. Resting oxygenation of rat and rabbit intestine: arteriolar and capillary contributions. *Am J Physiol Heart Circ Physiol* 269: H1342–H1348, 1995.
12. Boland EJ, Nair PK, Lemon DD, Olson JS, and Hellums JD. An in-vitro capillary system for studies on microcirculatory oxygen transport. *J Appl Physiol* 62: 791–797, 1987.
13. Bruttig SP and Joyner WL. Metabolic characteristics of cells cultured from umbilical blood vessels: comparison with 3T3 fibroblasts. *J Cell Physiol* 116: 173–180, 1983.
14. Buerk DG and Goldstick TK. Arterial wall oxygen consumption rate varies spatially. *Am J Physiol Heart Circ Physiol* 243: H948–H958, 1982.
15. Buerk DG and Goldstick TK. Spatial variations of aortic wall oxygen diffusion coefficient from transient polarographic measurements. *Ann Biomed Eng* 20: 629–646, 1992.
16. Buerk DG, Shonat RD, Riva CE, and Cranstoun SD. O_2 gradients and counter current exchange in the cat vitreous humor near retinal arterioles and venules. *Microvasc Res* 45: 134–148, 1993.
17. Buerk DG, Tsai AG, Intaglietta M, and Johnson PC. In vivo hamster skin fold tissue P_{O_2} measurements by phosphorescence quenching and recessed P_{O_2} microelectrodes are in agreement. *Microcirculation* 5: 219–225, 1998.
18. Burton AC. *Physiology and Biophysics of the Circulation*. Chicago, IL: Year Book, 1965.
19. Clark ER and Clark EL. Observations on changes in blood vascular endothelium in the living animal. *Am J Anat* 57: 285–301, 1935.
20. Clark LC. Electrochemical device for chemical analysis. US Patent 2,913,386, 1959.
21. Colantuoni A, Bertuglia S, and Intaglietta M. Effects of anesthesia on the spontaneous activity of the microvasculature. *Int J Microcirc Clin Exp* 3: 13–28, 1984.
22. Curtis SE, Vallet B, Winn MJ, Caufield JB, King CE, Chapler CK, and Cain SM. Role of vascular endothelium in O_2 extraction during progressive ischemia in canine skeletal muscle. *J Appl Physiol* 79: 1351–1360, 1995.

23. DILLER TE AND MIKIC BB. Oxygen diffusion in blood: a translational model of shear induced augmentation. *J Biomech Eng* 105: 67–72, 1980.
24. DULING BR. Microvascular responses to alterations in oxygen tension. *Circ Res* 31: 481–489, 1972.
25. DULING BR AND BERNE RM. Longitudinal gradients in periarteriolar oxygen tension. A possible mechanism for the participation of oxygen in the local regulation of blood flow. *Circ Res* 27: 669–678, 1970.
26. DULING BR, KUSCHINSKY W, AND WAHL M. Measurement of perivascular P_{O_2} in the vicinity of pial vessels in the cat. *Pflügers Arch* 383: 29–34, 1979.
27. DUTTA A AND POPEL AS. A theoretical analysis of intracellular oxygen diffusion. *J Theor Biol* 176: 433–445, 1995.
28. ELLSWORTH ML AND PITTMAN RN. Arterioles supply oxygen to capillaries by diffusion as well as by convection. *Am J Physiol Heart Circ Physiol* 258: H1240–H1243, 1990.
29. ELLSWORTH ML, PITTMAN RN, AND ELLIS CG. Measurement of hemoglobin oxygen saturation in capillaries. *Am J Physiol Heart Circ Physiol* 252: H1031–H1040, 1987.
30. ELLSWORTH ML, POPEL AS, AND PITTMAN RN. Assessment and impact of heterogeneity of convective oxygen transport parameters in capillaries of striated muscle: experimental and theoretical. *Microvasc Res* 35: 341–362, 1988.
31. ENDRICH B, ASAISHI K, GÖTZ A, AND MESSMER K. Technical report: a new chamber technique for microvascular studies in unanaesthetized hamsters. *Res Exp Med* 177: 125–134, 1980.
32. FAGRELL B, JÖRNESKOG G, AND INTAGLIETTA M. Disturbed microvascular reactivity and shunting: a major cause for diabetic complications. *Vasc Med* 4: 125–127, 1999.
33. FEDERSPIEL W AND POPEL A. A theoretical analysis of the effect of the particulate nature of blood on oxygen release in capillaries. *Microvasc Res* 32: 164–189, 1986.
34. FRANGOS JA, ESKIN SG, MCINTIRE LV, AND IVES CL. Flow effects on prostacyclin production in cultured human endothelial cells. *Science* 227: 1477–1479, 1985.
35. GALETTI P AND COLTON CK. Artificial lungs and blood gas exchange devices. In: *The Biomedical Engineering Handbook*, edited by Bronzino JD. Boca Raton, FL: CRC, 1995, p. 1879–1897.
36. GAYESKI TEJ AND HONIG CR. Oxygen gradients from sarcolema to cell interior in a red muscle at maximal oxygen consumption. *Am J Physiol Heart Circ Physiol* 251: H789–H799, 1986.
37. GAYESKI TEJ AND HONIG CR. Precapillary oxygen loss and arteriovenous oxygen diffusion shunt are below limit of detection in myocardium. *Adv Exp Med Biol* 248: 591–599, 1989.
38. GOLDSMITH HL, BELL DN, SPAIN S, AND MCINTOSH FA. Effect of red blood cells and their aggregates on platelets and white cells flowing in blood. *Biorheology* 36: 461–468, 1999.
39. GOLDSMITH HL, COKELET GR, AND GAEHTGENS P. Robin Fåhraeus: evolution of his concepts in cardivascular physiology. *Am J Physiol Heart Circ Physiol* 257: H1005–H1015, 1989.
40. GOLUB AS, POPEL AS, ZHENG L, AND PITTMAN RM. Analysis of phosphorescence decay in heterogeneous systems. Consequences of finite excitation flash duration. *Photochem Photobiol* 69: 624–632, 1999.
41. GOUGH D, SARGENT B, AND TSE P. A transparent oxygen sensor. *Ann Biomed Eng* 14: 153–161, 1986.
42. HARDER DR, NARAYANAN J, BIRKS EK, LAIRD JF, IMIG JD, LOMBARD JH, LANGE AR, AND ROMAN RJ. Identification of a putative microvasculature oxygen sensor. *Circ Res* 79: 54–61, 1996.
43. HELLUMS JD. The resistance to oxygen transport in the capillaries relative to that in the surrounding tissue. *Microvasc Res* 13: 131–136, 1977.
44. HELLUMS JD, NAIR PK, HUANG NS, AND OSHIMA N. Simulation of intraluminal gas transport processes in the microcirculation. *Ann Biomed Eng* 24: 1–24, 1996.
45. HELMLINGER G, ME, FERRARA N, HLATKY L, AND JAIN RK. Formation of endothelial cell networks. *Nature* 405: 139–141, 2000.
46. HLTAKY L AND ALPEN EL. Two-dimensional diffusion limited system for cell growth. *Cell Tiss Kinet* 18: 597–611, 1985.
47. HONIG CR AND GAYESKI TEJ. Precapillary oxygen loss and arteriovenous oxygen diffusion shunt are below limit of detection in myocardium. *Adv Exp Med Biol* 248: 591–599, 1989.
48. HONIG CR, GAYESKI TEJ, CLARK JA, AND CLARK PAA. Arteriovenous oxygen diffusion shunt is negligible in resting and working gracilis muscles. *Am J Physiol Heart Circ Physiol* 261: H2031–H2043, 1991.
49. HOWARD RO, RICHARDSON DW, SMITH MH, AND PATTERSON JL. Oxygen consumption of arterioles and venules studied by the Cartesian diver. *Circ Res* 26: 187–196, 1965.
50. INTAGLIETTA M AND JOHNSON PC:. Principles of capillary exchange. In: *Peripheral Circulation*, edited by Johnson PC. New York: Wiley, 1978.
51. INTAGLIETTA M, JOHNSON PC, AND WINSLOW RM. Microvascular and tissue oxygen distribution. *Cardiovasc Res* 32: 632–643, 1996.
52. INTAGLIETTA M AND ZWEIFACH BW. Microcirculatory basis of fluid exchange. In: *Advances in Biological and Medical Physics*. New York: Academic, 1973, vol. 15, p. 111–159.
53. IRIUCHIJIMA J AND KOIKE H. Carotid flow, intrasinusal pressure, and collateral flow during carotid occlusion. *Am J Physiol* 218: 876–879, 1970.
54. ITOH T, YAEGASHI K, KOSAKA T, KINOSHITA T, AND MORIMOTO T. In vivo visualization of oxygen transport in microvascular network. *Am J Physiol Heart Circ Physiol* 267: H2068–H2078, 1994.
55. IVANOV KP, DERRY AN, VOVENKO EP, SAMOILOV MO, AND SEMIONOV DG. Direct measurements of oxygen tension at the surface of arterioles, capillaries, and venules. *Pflügers Arch* 393: 118–120, 1982.
56. IVANOV KP, SOKOLOVA IB, AND VOVENKO EP. Oxygen transport in the rat brain cortex at normobaric hyperoxia. *Eur J Appl Physiol* 80: 582–587, 1999.
57. JOHNSON PC. Autoregulatory responses of cat mesenteric arterioles measured in vivo. *Circ Res* 22: 199–212, 1968.
58. KAWASHIRO T, NÜSSE W, AND SCHEID P. Determination of diffusivity of oxygen and carbon dioxide in respiring tissue: results in rat skeletal muscle. *Pflügers Arch* 359: 231–251, 1975.
59. KELLER KH AND FRIEDLANDER EK. The steady state transport of oxygen through hemoglobin solutions. *J Gen Physiol* 49: 663–679, 1966.
60. KERGER H, SALTZMAN DJ, GONZALES A, TSAI AG, VAN ACKERN K, WINSLOW RM, AND INTAGLIETTA M. Microvascular oxygen delivery and interstitial oxygenation during sodium pentobarbital. *Anesthesiology* 86: 372–386, 1997.
61. KERGER H, SALTZMAN DJ, MENGER MD, MESSMER K, AND INTAGLIETTA M. Systemic and subcutaneous microvascular P_{O_2} dissociation during 4-h hemorrhagic shock in conscious hamsters. *Am J Physiol Heart Circ Physiol* 270: H827–H836, 1996.
62. KERGER H, TORRES FILHO IP, RIVAS M, WINSLOW RM, AND INTAGLIETTA M. Systemic and subcutaneous microvascular oxygen tension in conscious syrian golden hamsters. *Am J Physiol Heart Circ Physiol* 267: H802–H810, 1995.
63. KESSLER M, HOPER J, AND KRUMME BA. Monitoring of tissue perfusion and cellular function. *Anesthesiology* 45: 184–197, 1976.
64. KJELLSTROM BT, ORTENWALL P, AND RISBERG R. Comparison of oxidative metabolism in vitro in endothelial cells from different species and vessels. *J Cell Physiol* 132: 578–580, 1987.
65. KOBAYASHI H, PELSTRE B, PIIPER J, AND SCHEIF P. Significance of Bohr effect for tissue oxygenation in a model with counter current blood flow. *Respir Physiol* 76: 227–288, 1989.
66. KOBAYASHI H AND TAKIZAWA N. Oxygen saturation and pH changes in cremaster microvessels of the rat. *Am J Physiol Heart Circ Physiol* 270: H1453–H1461, 1996.
67. KROGH A. The number and distribution of capillaries in muscle with the calculation of the oxygen pressure necessary for supplying the tissue. *J Physiol* 52: 409–515, 1918.
68. KRUEZER F. Oxygen supply to tissues: the Krogh model and its assumptions. *Experientia* 38: 1415–1426, 1982.
69. KUEHL KS, BRUTTIG SP, SINGER DV, RUBIO R, AND BERNE RM. Growth of aortic vascular smooth muscle cells in lowered oxygen tension. *Cell Tissue Res* 216: 591–602, 1981.
70. KUO L AND PITTMAN RN. Effect of hemodilution on oxygen transport in arteriolar networks of hamster striated muscle. *Am J Physiol Heart Circ Physiol* 254: H331–H338, 1988.
71. KUSZA K, LIEMIONOW M, NALBANTOGLU U, HAYES J, AND WONG KC. Microcirculatory response to halothane and isoflurane anesthesia. *Ann Plast Surg* 43: 57–66, 1999.
72. LASH JM AND BOHLEN HG. Perivascular and tissue P_{O_2} in contracting

rat spinotrapezius muscle. *Am J Physiol Heart Circ Physiol* 252: H1192–H1202, 1987.
73. Leunig M, Yuan F, Menger MD, Boucher Y, Goetz AE, Messmer K, and Jain RK. Angiogenesis, microvascular architecture, microhemodyanmics and interstitial fluid pressure during early growth of human adenocarcinoma LS174T in SCID mice. *Cancer Res* 52: 6553–6560, 1992.
74. Levasseur JE and Kontos HA. Effects of anesthesia on cerebral arteriolar responses to hypercapnia. *Am J Physiol Heart Circ Physiol* 257: H85–H88, 1989.
75. Levasseur JE, Wei EP, Raper EJ, Kontos HA, and Patterson JL Jr. Detailed description of a cranial window technique for acute and chronic experiments. *Stroke* 6: 308–317, 1975.
76. Li C and Jackson RM. Reactive species mechanisms of cellular hypoxia-reoxygenation injury. *Am J Physiol Cell Physiol* 282: C227–C241, 2002.
77. Loeb A, Godeny I, and Longnecker DE. Anesthetics alter relative contributions of NO and EDHF in rat cremaster muscle microcirculation. *Am J Physiol Heart Circ Physiol* 273: H618–H627, 1997.
78. Marshall JM and Davies WR. The effects of acute and chronic systemic hypoxia on muscle oxygen supply and oxygen consumption. *Exp Physiol* 84: 57–68, 1999.
79. Maude AD and Whitmore RL. The wall effect and the viscometry of suspension. *Br J Appl Physiol* 7: 98–102, 1956.
80. Messina EJ, Sun D, Koller A, Wolin MS, and Kaley G. Increase in oxygen tension evokes arteriolar constriction by inhibiting endothelial prostaglandin synthesis. *Microvasc Res* 8: 151–160, 1994.
81. Middleman S. *Transport Phenomena in the Cardiovascular System*. New York: Wiley Interscience, 1972.
82. Motterlini R, Kerger H, Green CJ, Winslow RM, and Intaglietta M. Depression of endothelial and smooth muscle cell oxygen consumption by endotoxin. *Am J Physiol Heart Circ Physiol* 275: H776–H782, 1998.
83. Nair PK, Huang NS, Hellums JD, and Olson JS. A simple method for prediction of oxygen transport rates by flowing blood in large capillaries. *Microvasc Res* 39: 203–211, 1990.
84. Niinikoski J, Hughen C, and Hunt T. Oxygen tensions in the aortic wall of normal rabbits. *Atherosclerosis* 17: 353–359, 1973.
85. Papenfuss HD, Gross JF, Intaglietta M, and Treese FA. A transparent access chamber for the rat dorsal skin fold. *Microvasc Res* 18: 311–318, 1979.
86. Parker JC, Perry MA, and Taylor AE. Permeability of the vascular barrier. In: *Edema*, edited by Staub NC and Taylor AE. New York: Raven, 1984, p. 143–188.
87. Paul RJ. Chemical energetics of vascular smooth muscle. In: *Handbook of Physiology. The Cardiovascular System. Vascular Smooth Muscle*. Bethesda, MD: Am Physiol Soc, 1980, sect. 2, vol. II, chapt. 9, p. 201–235.
88. Paul RJ. Smooth muscle energetics and theories of cross-bridge regulation. *Am J Physiol Cell Physiol* 258: C369–C375, 1990.
89. Pittman RN. Influence of microvascular architecture on oxygen diffusion from arteriolar networks. *Microcirculation* 2: 1–18, 1995.
90. Pittman RN and Duling BR. Measurement of percent hemoglobin in the microvasculature. *J Appl Physiol* 38: 321–327, 1975.
91. Pittman RN and Duling BR. Effects of altered carbon dioxide tension on hemoglobin oxygenation in the hamster cheek pouch microvessels. *Microvasc* Res 13: 211–224, 1977.
92. Plattner H and Bachmann L. Cryofixation: a tool in biological ultrastructural research. *Int Rev Cytol* 79: 237–303, 1982.
93. Pohl U and Busse R. Hypoxia stimulates release of endothelium-derived relaxing factor. *Am J Physiol Heart Circ Physiol* 256: H1595–H1600, 1989.
94. Popel AS. Theory of oxygen transport to tissue. *Crit Rev Biomed Eng* 17: 257–321, 1989.
95. Popel AS, Pittman RN, and Ellsworth ML. Rate of oxygen loss from arterioles is an order of magnitude than expected. *Am J Physiol Heart Circ Physiol* 256: H921–H924, 1988.
96. Prewitt RL and Johnson PC. The effect of oxygen on arteriolar red cell velocity and capillary density in the rat cremaster muscle. *Microvasc Res* 12: 59–70, 1976.
97. Reinhold HS. Reoxygenation of tumors in "sandwich" chambers. *Eur J Cancer* 15: 481–489, 1979.
98. Rhodin JA. Ultrastructure of mammalian venous capillaries, venules, and small collecting veins. *J Ultrastruct Res* 25: 452–500, 1968.
99. Richmond KN, Shonat RD, Lynch RM, and Johnson PC. Critical P_{O_2} of skeletal muscle in vivo. *Am J Physiol Heart Circ Physiol* 277: H1831–H1840, 1999.
100. Roth AC and Wade K. The effects of transmural transport in the microcirculation: a two gas species model. *Microvasc Res* 32: 64–83, 1986.
101. Rubin MJ and Bohlen HG. Cerebral vascular autoregulation of blood flow and tissue P_{O_2} in diabetic rats. *Am J Physiol Heart Circ Physiol* 249: H540–H546, 1985.
102. Saltzman D, DeLano FA, and Schmid-Schönbein GW. The microvasculature in skeletal muscle. VI. Adrenergic innervation of arterioles in normotensive and spontaneously hypertensive rats. *Microvasc Res* 44: 263–273, 1992.
103. Sandinson JC. Observations on the growth of blood vessels as seen in the transparent chamber introduced in the rabbit's ear. *Am J Physiol* 41: 475–496, 1928.
104. Santilli SM, Stevens RB, Anderson JG, Payne WD, and Caldwell MD. Transarterial wall oxygen gradients at the dog carotid bifurcation. *Am J Physiol Heart Circ Physiol* 268: H155–H161, 1995.
105. Santilli SM, Tretinyak AS, and Lee ES. Transarterial wall gradients at the development site of an intra-arterial stent in the rabbit. *Am J Physiol Heart Circ Physiol* 279: H1518–H1525, 2000.
106. Schneiderman G and Goldstick TK. Oxygen electrode design criteria and performance characterstics: recessed cathode. *J Appl Physiol* 45: 145–154, 1978.
107. Schumacher J, Porksen M, and Klotz KF. Effects of isoflurane, enflurane and halothane on skeletal muscle microcirculation in the endotoxemic rat. *J Crit Care* 16: 1–7, 2001.
108. Secomb TW and Hsu R. Simulation of O_2 transport in skeletal muscle: diffusive exchange between arterioles and capillaries. *Am J Physiol Heart Circ Physiol* 267: H1214–H1221, 1994.
109. Seiyama A, Tanaka S, Kosaka H, and Shiga T. O_2 transfer from single microvessels to acinar cells in secretin-stimulated pancreas of rat. *Am J Physiol Heart Circ Physiol* 270: H1704–H1711, 1996.
110. Shen W, Hintze TH, and Wolin MS. Nitric oxide. An important signaling mechanism between vascular endothelium and parenchymal cells in the regulation of oxygen consumption. *Circulation* 92: 3505–3512, 1995.
111. Shen W, Xu X, Ochoa M, Zhao G, Wolin MS, and Hintze TH. Role of nitric oxide in the regulation of oxygen consumption in conscious dogs. *Circ Res* 75: 1086–1095, 1994.
112. Shibata M, Ichioka S, Ando J, and Kamiya A. Microvascular and interstitial P_{O_2} measurements in rat skeletal muscle by phosphorescence quenching. *J Appl Physiol* 91: 321–327, 2001.
113. Shonat RD and Johnson PC. Oxygen tension gradients and heterogeneity in venous microcirculation: a phosphorescence quenching study. *Am J Physiol Heart Circ Physiol* 272: H2233–H2240, 1997.
114. Shonat RD, Richmond KN, and Johnson PC. Phosphorescence quenching and the microcirculation: an automated, multipoint oxygen tension measuring instrument. *Rev Sci Instr* 66: 5075–5084, 1995.
115. Shonat RD, Wilson DF, Riva CE, and Pawlowski M. Oxygen distribution in the retinal and choroidal vessels of the cat as measured by a new phosphorescence imaging method. *Applied Optics* 31: 3711–3718, 1992.
116. Silver IA. Some observations on the cerebral cortex with an ultramicro, membrane-covered, oxygen electrode. *Med Electron Biol Eng* 3: 377–387, 1965.
117. Sinaasappel M, van Iterson M, and Ince C. Microvascular oxygen pressure in the pig intestine during hemorrhagic shock and resuscitation. *J Physiol* 514: 245–253, 1999.
118. Smith TL, Osborne SW, and Hutchins PM. Long-term micro- and macrocirculatory measurements in conscious rats. *Microvasc Res* 29: 360–370, 1985.
119. Steenbergen JM, Lash JM, and Bohlen HG. Role of lymphatic system in glucose absorption and the accompanying microvascular hyperemia. *Am J Physiol Gastrointest Liver Physiol* 267: G529–G535, 1994.
120. Stein JC, Ellis CG, and Ellsworth ML. Relationship between capillary and systemic venous P_{O_2} during nonhypoxic and hypoxic

ventilation. *Am J Physiol Heart Circ Physiol* 265: H537–H542, 1993.
121. SULLIVAN SM AND JOHNSON PC. Effect of oxygen on arteriolar dimensions and blood flow in cat sartorius muscle. *Am J Physiol Heart Circ Physiol* 241: H547–H556, 1981.
122. SUSSMAN I, CARSON MP, MCCALL AL, SCHULTZ V, RUDERMAN NB, AND TORNHEIM K. Energy state of of bovine cerebral microvessels: comparison of isolation methods. *Microvasc Res* 35: 167–178, 1988.
123. SWAIN DP AND PITTMAN RN. Oxygen exchange in the microcirculation of hamster cremaster muscle. *Am J Physiol Heart Circ Physiol* 256: H247–H255, 1989.
124. TATEISHI N, MEADA N, AND SHIGA T. A method for measuring the rate of oxygen release from single microvessels. *Circ Res* 70: 812–819, 1992.
125. TEISSEIRE BP, SOULARD CD, HERIGAULT RA, LECLERC LL, AND LAVER MB. Effects of chronic changes in hemoglobin-O_2 affinity in rats. *J Appl Physiol* 46: 816–822, 1979.
126. TONG AC, DI MARIA CA, RATTIGAN S, AND CLARK MG. Na^+ channel and Na^+-K^+ ATPase involvement in norepinephrine- and veratridine-stimulated metabolism in perfused rat hind limb. *Can J Physiol Pharm* 77: 250–257, 1999.
127. TONG AC, RATTIGAN S, DORA KA, AND CLARK MG. Vasoconstrictor mediated increase in muscle resting thermogenesis is inhibited by membrane stabilizing agents. *Can J Physiol Pharm* 75: 763–771, 1997.
128. TORRES FILHO IP, FAN Y, INTAGLIETTA M, AND JAIN RK. Non-invasive measurement of microvascular and interstitial oxygen profiles in a human tumor in SCID mice. *Proc Natl Acad Sci USA* 91: 2081–2085, 1994.
129. TORRES FILHO IP AND INTAGLIETTA M. Microvessel P_{O_2} measurements by phosphorescence decay method. *Am J Physiol Heart Circ Physiol* 265: H1434–H1438, 1993.
130. TORRES FILHO IP, KERGER H, AND INTAGLIETTA M. P_{O_2} measurements in arteriolar networks. *Microvasc Res* 51: 202–212, 1996.
131. TSAI AG. Influence of cell-free hemoglobin on local tissue perfusion and oxygenation after acute anemia after isovolemic hemodilution. *Transfusion* 41: 1290–1298, 2001.
132. TSAI AG, FRIESENECKER B, MAZZONI MC, KERGER H, BUERK DG, JOHNSON PC, AND INTAGLIETTA M. Microvascular and tissue oxygen gradients in the rat mesentery. *Proc Natl Acad Sci* 95: 6590–6595, 1998.
133. TSAI AG, KERGER H, AND INTAGLIETTA M. Microcirculatory consequences of blood substitution with $\alpha\alpha$-hemoglobin. In: *Blood Substitutes. Physiological Basis of Efficacy*, edited by Winslow RM, Vandegriff KD, and M Intaglietta M. Boston, MA: Birkhäuser, 1995, p. 155–174.
134. ULRICH S, HILPERT P, AND BARTELS H. Ueber die Atmungsfunktion des Blutes von Spitzmausen, weissen Mausen und syrischen Goldhamstern. *Arch Ges Physiol* 277: 150–165, 1963.
135. VADAPALLI A, PITTMAN RN, AND POPEL AS. Estimating oxygen transport resistance of the microvascular wall. *Am J Physiol Heart Circ Physiol* 279: H657–H671, 2000.
136. VANDERKOOI JM, MANIARA G, GREEN TJ, AND WILSON DF. An optical method for measurement of dioxygen concentration based on quenching of phosphorescence. *J Biol Chem* 262: 5476–5482, 1987.
137. VINOGRADOV SA AND WILSON DF. Phosphorescence lifetime analysis with a quadratic programming algorithm for determining quencher distributions in heterogeneous systems. *Biophys J* 67: 2048–2059, 1994.
138. VOVENKO EP. Distribution of oxygen tension on the surface of arterioles, capillaries and venules of brain cortex and in tissue in normoxia: an experimental study on rats. *Pflügers Arch* 437: 617–623, 1999.
139. WAGNER PD. Diffusive resistance to O_2 transport in muscle. *Acta Physiol Scand* 168: 609–614, 2000.
140. WEIBEL ER. *The Pathway for Oxygen*. Cambridge, MA: Harvard Univ. Press, 1984.
141. WHALEN WJ, RILEY J, AND NAIR P. A microelectrode for measuring intracellular P_{O_2}. *J Appl Physiol* 23: 789–794, 1967.
142. WILSON DF. Measuring oxygen using oxygen dependent quenching of phosphorescence: a status report. *Adv Exp Med Biol* 333: 225–232, 1993.
143. WILSON DF, PASTUSZKO A, DIGIACOOMO JE, PAWLOWSKI M, SHNEIDERMAN R, AND DELIVORIA-PAPADOPULOS M. Effect of hyperventilation on oxygenation of the brain cortex of newborn piglets. *Adv Exp Med Biol* 333: 225–232, 1991.
144. WITTENBERG BA AND WITTENBERG JB. Transport of oxygen in muscle. *Annu Rev Med* 51: 857–878, 1981.
145. YAEGASHI K, TOSHIYUKI I, KOSAKA T, FUKUSHIMA H, MORIMOTO T. Diffusivity of oxygen in microvascular beds as determined from P_{O_2} distribution maps. *Am J Physiol Heart Circ Physiol* 270: H1390–H1397, 1996.
146. YE JM, COLQUHOUN EQ, AND CLARK MG. A comparison of vasopressin and noradrenaline on oxygen uptake by perfused rat hind limb, intestine, and mesenteric arcade suggests that it is part due to contractile work by blood vessels. *Gen Pharmacol* 21: 805–810, 1990.
147. ZHENG L, GOLUB AS, AND PITTMAN RN. Determination of P_{O_2} and its heterogeneity in single capillaries. *Am J Physiol Heart Circ Physiol* 271: H365–H372, 1996.
148. ZYDNEY AL AND COLTON CK. Augmented solute transport in the shear flow of a concentrated suspension. *Physico Chem Hydrodynam* 10: 77–96, 1988.